Physica D 485 (2026) 135037

Contents lists available at ScienceDirect

Physica D

journal homepage: www.elsevier.com/locate/physd

A general formulation of the survival problem in a power-law reaction–diffusion model: Emergence of a critical parameter

Rafael de la Rosa *, Elena Medina

Departamento de Matemáticas, Facultad de Ciencias, Universidad de Cádiz, 11510 Puerto Real, Cádiz, Spain

ARTICLE INFO

Communicated by Victor M. Perez-Garcia

Keywords:
Population dynamics
Critical parameter
Initial distributions
Boundary conditions
Numerical analysis

ABSTRACT

The survival of a population confined within a bounded habitat is a classical problem, traditionally analyzed in terms of the habitat size. In the linear case, persistence is ensured when the domain length exceeds a critical size l_c. In nonlinear models, however survival conditions become considerably more complex and may even take less intuitive forms, such as $l \leq l_c$. In this context, Colombo and Anteneodo (2018) studied the power-law reaction–diffusion model $u_t = D(u^{\nu-1}u_x)_x + a u^{\mu}$, with $\mu, \nu > 0$, accompanied by hostile boundary conditions, determining survival thresholds in terms of habitat size for initially homogeneous populations.

In this paper, we propose a general formulation of the persistence question by rewriting the power-law reaction–diffusion model in terms of suitable nondimensional variables. This approach reveals that persistence can be naturally expressed through a parameter $Q := \frac{a}{D} l^{-\mu+\nu+2} n_0^{\mu-\nu}$. We show that there exists a critical value Q_c depending on μ, ν and the initial distribution, such that survival occurs whenever $Q \geq Q_c$. This more intuitive condition reconciles the various survival criteria within a unified framework.

To further explore this condition, we analyze two one-parameter families of initial distributions, including the homogeneous case, and apply a finite-difference scheme to estimate Q_c. Conversely, for given model parameters μ, ν, l, n_0, and the growth and diffusion coefficients a and D (and consequently the value of Q) we use the numerical algorithm to determine how concentrated the initial distribution must be to ensure population survival.

1. Introduction

The analysis of the evolution of a population is a crucial topic in fields such as biology, ecology, medicine and agriculture. One of the main concerns is the survival of the species, and more specifically, the conditions that the habitat has to fulfill for the persistence of a population. Since the pioneering Skellam's work [1], the effect of the size of the habitat on the fate of the population has been thoroughly investigated [2–17]. The problem is usually posed in terms of diffusion–reaction equations, however, convective terms are usually included (see, for example, [8] where the effects of the wind or water currents are taken into account, [14] where the extinction velocity of bacteria colonies under forced convection is analyzed, [11] and more recently [6]). In these models the effect of the boundary can be completely hostile, i.e., individuals die if they reach the habitat boundary, and consequently, Dirichlet homogeneous boundary conditions are imposed. Nevertheless, different degrees to which the region outside the patch is lethal are also considered. Some of the papers devoted to populations in bounded habitats with only partially hostile boundaries are: [12] where the width of the partially hostile surrounding region to avoid an outbreak state is studied, [18] where the optimal location of a protective zone is investigated, [3] for a predator–prey model, [13] for a two-sex population model, or [16] for a competition model. Other alternative models are discussed in [5] where the patch size is allowed to depend on time, [7] where the diffusion coefficient is, in general, space dependent, or [6] where the models include the existence of preferred regions in the habitat. The dependence of this critical size with the geometry of the domain has been addressed for example in [8,19]. Experimental confirmation of these results is provided in [15] for an E-coli population in a quasi-one dimensional habitat.

Among the different modeling approaches, the linear case has been extensively studied, concluding the existence of a critical patch size such that the population survives for larger habitat sizes whereas it gets extinct for smaller ones. Moreover, the critical size depends neither on the total initial population nor on the shape of its initial distribution.

More recently, attention has shifted toward nonlinear models, in which the mechanisms determining population persistence exhibit a wider variety of behaviors. Notably, in some situations, species persistence may require a habitat smaller than a critical size. Moreover,

* Corresponding author.
E-mail addresses: rafael.delarosa@uca.es (R. de la Rosa), elena.medina@uca.es (E. Medina).

https://doi.org/10.1016/j.physd.2025.135037
Received 9 September 2025; Received in revised form 3 November 2025; Accepted 13 November 2025
Available online 15 November 2025

unlike in the linear case, the persistence conditions depend on the total initial population and on the spatial shape of its initial distribution.

This paradoxical behavior was previously discussed in [4], where Colombo and Anteneodo consider the persistence of a population which evolves according to the reaction–diffusion equation

$$u_t = D\,(u^{\nu-1}\,u_x)_x + a\,u^{\mu}, \tag{1}$$

where both diffusion and growth coefficients are not constant but depend on the concentration through a power of the density with a specific exponent [20]. The population is supposed to be confined in a habitat of size l, such that outside the habitat there are not appropriate life conditions for the individuals so that if they reach the boundary, they die. Thus, the boundary conditions can be written as

$$u\left(-\frac{l}{2},t\right) = u\left(\frac{l}{2},t\right) = 0, \tag{2}$$

and the initial distribution is assumed to be homogeneous with a total initial population n_0, i.e.

$$u(x,0) = \frac{n_0}{l}. \tag{3}$$

The results in [4] can be summarized as

1. For $\mu < \nu$ the population survives independently of the habitat size l and the total initial population n_0. Moreover, it reaches a steady state.
2. For $\mu = \nu$, there exists a critical habitat size l_c which does not depend on the total initial population. The population goes extinct for smaller habitat sizes whereas it grows unboundedly for larger habitat sizes.
3. For $\mu \in (\nu, \nu+2)$, the survival condition is similar as in the previous case but the critical habitat size does depend on the total initial population through a factor of the form $n_0^{\frac{\nu-\mu}{2+\nu-\mu}}$.
4. For $\mu > \nu+2$, there also exists a critical habitat size depending on the total initial population through a factor $n_0^{\frac{\nu-\mu}{2+\nu-\mu}}$. However, in this case the population goes extinct for larger habitat sizes while it survives (with unbounded growth) for smaller habitat sizes.

In this work, we propose a reformulation of the reaction–diffusion problem (1)–(2) using suitable nondimensional variables, focusing on the case $\mu > \nu$ (regime of conditional survival). This change of variables not only simplifies the analysis but also resolves the paradoxical behavior previously observed in the critical habitat problem, leading to a more natural and intuitive persistence condition. Specifically, population survival occurs whenever $Q \geq Q_c$ where

$$Q := \frac{a}{D}\,l^{-\mu+\nu+2}\,n_0^{\mu-\nu}, \tag{4}$$

and the critical value Q_c depends on the exponents μ and ν as well as on the initial distribution $u_0(x)$.

Having established this general formulation, we next investigate how the critical value Q_c depends on the initial distribution of the population. This can be a relevant problem when a habitat with a given size has to be repopulated by a certain endangered species and only a fixed amount of individuals are available.

To explore this dependence, we consider two one-parameter families of initial distributions, each one corresponding to a fixed total initial population n_0. The parameter $\alpha \geq 0$ controls the spatial concentration of the population: when $\alpha = 0$ the initial distribution is homogeneous, whereas increasing values of α lead to progressively more concentrated distributions. In the first family, the distributions are symmetric with respect to the center of the habitat, while in the second one the population is initially concentrated around a point displaced toward the right boundary.

We apply a numerical algorithm to analyze how the critical value Q_c depends on the exponents μ and ν, and on the parameter α in the initial condition. Conversely, given the model parameters, i.e., the exponents μ and ν, the habitat size l, the total population n_0 and the growth and diffusion coefficients a and D (and consequently the value of Q) we use the numerical algorithm to estimate the value of the parameter α or more qualitative how concentrated the initial population should be to ensure survival.

Altogether, this formulation provides a coherent framework that reconciles the different survival criteria, showing that they can all be expressed through the general condition $Q \geq Q_c$.

This paper is organized as follows. In Section 2, we discuss the model and present the two families of one-parametric initial distributions. In Section 3, we show that the use of suitable nondimensional variables leads to the general and more intuitive persistence condition $Q \geq Q_c$, where Q is given by (4) and Q_c is a critical value depending on the exponents μ and ν and the initial distribution parameter α. In Section 4, we will make use of the numerical algorithm to examine the influence of the exponents μ and ν as well as the initial distribution parameter α on the critical value $Q_c(\mu,\nu,\alpha)$. This algorithm will be also used to determine the minimum value of the initial distribution parameter that guarantees the persistence of the population. The final part of Section 4 translates these findings into conditions involving the habitat size and total population, whose dependence proves rather intricate, and confirms the consistency with the results in [4] for $a = D = 1$ and homogeneous initial distributions. In Section 5 we present some concluding remarks. The numerical implementation of the finite-difference method is presented in Appendix A. Appendix B is devoted to the determination of the total population $N(t)$, obtained via the trapezoidal rule, which serves as the main indicator of persistence or extinction. Finally, Appendix C includes some additional results that further illustrate our analysis.

2. The model

The reference framework for our analysis is the reaction–diffusion equation (1) introduced in [4]. The main properties of (1) as a dynamical population model, along with its ecological implications, are as follows:

- The diffusion term $(D\,u^{\nu-1}\,u_x)_x$ is, in general, nonlinear. Nonlinear diffusion terms, particularly power-law diffusion coefficients, have been widely used in dynamical population models. On the one hand, the case $\nu > 1$ corresponds to species that, to avoid extinction, exhibit a low dispersal rate at low concentrations or to species provided with regulatory mechanisms to reduce overcrowding: large populations tend to a faster dispersion [21–23]. On the other hand, social species such as insects tend to cluster as a survival strategy [24,25], which corresponds to $0 < \nu < 1$. This behavior is also observed in invading species [26]. Incidentally, nonlinear diffusion processes are also relevant in other contexts, such as transport in porous media [27], interstellar diffusion [28] or energy spreading in nonlinear disordered lattices [29].
- The reaction term $a\,u^{\mu}$ corresponds to a growth rate depending on the population density $a\,u^{\mu-1}$, which is particularly relevant at low concentrations. If $\mu > 1$, the term describes a population that, at low densities, experiences difficulties in reproduction and grows very slowly. This phenomenon is known as Allee effect [30]. The opposite behavior, $\mu < 1$, is also possible in species, for instance zooplankton, which are capable to fit their reproduction mechanisms depending on the population density [31].
- The intraspecific competition term has been neglected. Typical reasons to remove this term [32] include: presence of abundant resources, human intervention (for instance, population in an experimental environment where nutrients are being continuously supplied) or social animal populations, where the cooperative behavior may significantly reduce the effect of the intraspecific competition for resources.

Eq. (1) with hostile (Dirichlet) boundary conditions (2) and the initial condition $u(x,0) = u_0(x)$ lead us to the problem

$$\begin{cases} u_t = D\,(u^{\nu-1}\,u_x)_x + a\,u^{\mu}, & x \in \left[-\frac{l}{2},\frac{l}{2}\right],\ t > 0, \\ u\left(-\frac{l}{2},t\right) = u\left(\frac{l}{2},t\right) = 0, & t > 0, \\ u(x,0) = u_0(x), & x \in \left[-\frac{l}{2},\frac{l}{2}\right], \end{cases} \tag{5}$$

where the total initial population is given by

$$\int_{-\frac{l}{2}}^{\frac{l}{2}} u_0(x)\,dx = n_0. \tag{6}$$

In order to analyze the dependence of the survival condition with the initial distribution we consider two families of one-parametric initial distributions $u_0(x;\alpha)$ corresponding to a habitat size l, a total population n_0 and a certain parameter α such that:

- α takes non-negative values.
- $u_0(x;0) = \frac{n_0}{l}$, i.e., for $\alpha = 0$ the initial distribution is the homogeneous initial distribution.
- As α grows the initial distribution is more and more concentrated in a small neighborhood of a point of the habitat size (see Figs. 1 and 2).

The first family of initial conditions we consider is given by

$$u_{0,1}(x;\alpha) = \frac{1}{B(1+\alpha,1+\alpha)}\left(\frac{1}{4} - \frac{x^2}{l^2}\right)^{\alpha}\frac{n_0}{l}, \quad \alpha \geq 0, \tag{7}$$

where $B(a,b)$ denotes the Beta function. Note that $u_{0,1}(x;0) = n_0/l$ corresponds to the homogeneous distribution and as α increases, the initial distributions tend to concentrate near the origin. Furthermore, we consider a second family of initial conditions given by

$$u_{0,2}(x;\alpha) = \frac{1}{B(1+\gamma(\alpha),1+2\gamma(\alpha))}\left(\left(\frac{1}{2}-\frac{x}{l}\right)\left(\frac{1}{2}+\frac{x}{l}\right)^2\right)^{\gamma(\alpha)}\frac{n_0}{l}, \quad \alpha \geq 0, \tag{8}$$

where $\gamma(\alpha)$ is determined as the unique solution of the equation

$$4^{\alpha}B(1+\alpha,1+\alpha) = \left(\frac{27}{4}\right)^{\gamma} B(1+\gamma,1+2\gamma). \tag{9}$$

Note that, according to (9) $\gamma(0) = 0$, so that $u_{0,2}(x,0) = n_0/l$. Moreover, $u_{0,2}(\cdot;\alpha)$ reaches its maximum at $x = l/6$, and consequently,

$$u_{0,2,max}(\alpha) = u_{0,2}\left(\frac{l}{6};\alpha\right) = \left(\frac{4}{27}\right)^{\gamma(\alpha)}\frac{1}{B(1+\gamma(\alpha),1+2\gamma(\alpha))}\frac{n_0}{l}. \tag{10}$$

On the other hand, the first family of initial distributions is symmetric with respect to the midpoint of the habitat, $x = 0$, so that

$$u_{0,1,max}(\alpha) = u_{0,1}(0;\alpha) = \left(\frac{1}{4}\right)^{\alpha}\frac{1}{B(1+\alpha,1+\alpha)}\frac{n_0}{l}. \tag{11}$$

Thus, for the choice of $\gamma(\alpha)$ given by Eq. (9), both families of initial distributions satisfy

$$u_{0,1,max}(\alpha) = u_{0,2,max}(\alpha). \tag{12}$$

We plot the ratios of the initial distributions $u_{0,1}(\cdot;\alpha)$ (respectively $u_{0,2}(\cdot;\alpha)$) to the homogeneous initial distribution n_0/l in Fig. 1 (respectively Fig. 2) for the values $\alpha = 0$ (green, homogeneous distribution), $\alpha = 1$ (brown), $\alpha = 10$ (gray), $\alpha = 100$ (blue) and $\alpha = 500$ (red).

3. Nondimensional reformulation and emergence of the critical parameter

We now reformulate the problem (5)–(6) in nondimensional variables, which provides a more general framework for the analysis of population survival. The nondimensional representation allows us to identify the relevant combinations of parameters and to establish a unified criterion for persistence.

If we rescale x by using the habitat size, i.e.

$$X = \frac{x}{l}, \tag{13}$$

then, it is possible to remove a and D from the reaction–diffusion equation provided that $\mu \neq \nu$, by rescaling t and u as

$$T = a\left(\frac{D}{a\,l^2}\right)^{\frac{\mu-1}{\mu-\nu}} t, \quad \rho = \left(\frac{D}{a\,l^2}\right)^{-\frac{1}{\mu-\nu}} u. \tag{14}$$

In this case, problem (5) takes the form

$$\begin{cases} \rho_T = (\rho^{\nu-1}\,\rho_X)_X + \rho^{\mu}, & X \in \left[-\frac{1}{2},\frac{1}{2}\right],\ T > 0, \\ \rho\left(-\frac{1}{2},T\right) = \rho\left(\frac{1}{2},T\right) = 0, & T > 0, \\ \rho(X,0) = \rho_0(X), & X \in \left[-\frac{1}{2},\frac{1}{2}\right], \end{cases} \tag{15}$$

where

$$\rho_0(X) = \left(\frac{D}{a\,l^2}\right)^{-\frac{1}{\mu-\nu}} u_0\,(l\,X), \tag{16}$$

which satisfies

$$\int_{-\frac{1}{2}}^{\frac{1}{2}} \rho_0(X)\,dX = N_0, \tag{17}$$

with

$$N_0 = \left(\frac{D}{a\,l^2}\right)^{-\frac{1}{\mu-\nu}}\frac{n_0}{l}. \tag{18}$$

The survival condition for (15) with $\rho_0(X)$ satisfying (17) takes the form $N_0 \geq N_{0,c}$ where $N_{0,c}$ is a critical value depending on the growth exponent μ, the diffusion exponent ν and the particular choice of the initial condition $\rho_0(X)$ satisfying (17). If we assume that we are considering a family of initial data satisfying (17) and depending on a certain set of parameters $\Lambda = \{\alpha_1,\alpha_2,\ldots,\alpha_K\}$ the survival condition can be written as

$$N_0 \geq N_{0,c}(\mu,\nu,\Lambda). \tag{19}$$

On the other hand, if $\nu = \mu$, in order to remove the parameters from the diffusion–reaction equation we take into account (6) and use the variables

$$X = \sqrt{\frac{a}{D}}\,x, \quad T = a\left(\frac{a}{D}\right)^{\frac{\mu-1}{2}} n_0^{\mu-1}\,t, \quad \rho = \left(\frac{a}{D}\right)^{-\frac{1}{2}}\frac{u}{n_0}. \tag{20}$$

In terms of (20), problem (5) takes the form

$$\begin{cases} \rho_T = (\rho^{\mu-1}\,\rho_X)_X + \rho^{\mu}, & X \in \left[-\frac{L}{2},\frac{L}{2}\right],\ T > 0, \\ \rho\left(-\frac{L}{2},T\right) = \rho\left(\frac{L}{2},T\right) = 0, & T > 0, \\ \rho(X,0) = \rho_0(X), & X \in \left[-\frac{L}{2},\frac{L}{2}\right], \end{cases} \tag{21}$$

where

$$L = \sqrt{\frac{a}{D}}\,l, \tag{22}$$

and

$$\rho_0(X) = \sqrt{\frac{D}{a}}\,\frac{1}{n_0}\,u_0\left(\sqrt{\frac{D}{a}}X\right), \tag{23}$$

that satisfies

$$\int_{-\frac{L}{2}}^{\frac{L}{2}} \rho_0(X)\,dX = 1. \tag{24}$$

Colombo and Anteneodo in [4] provided numerical evidence that the survival condition for (21) is given by

$$L \geq \frac{\pi}{\sqrt{\mu}}, \tag{25}$$

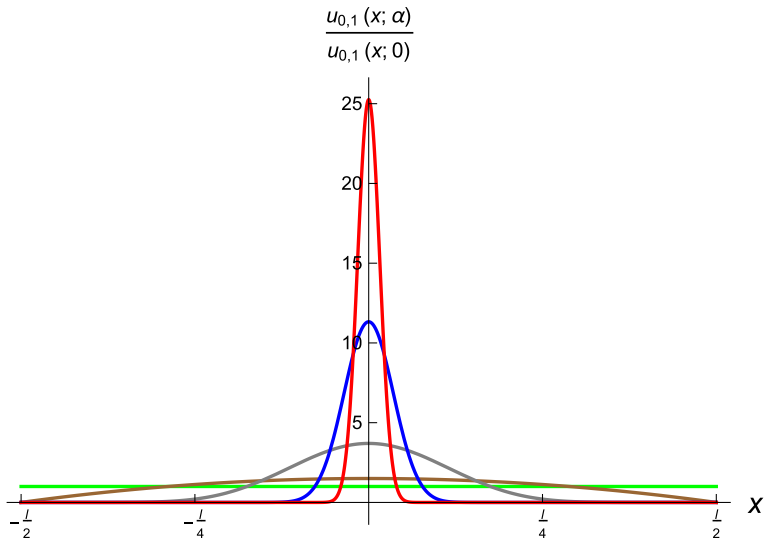

Fig. 1. Initial distributions (7) for the values $\alpha = 0$ (green, homogeneous distribution), $\alpha = 1$ (brown), $\alpha = 10$ (gray), $\alpha = 100$ (blue) and $\alpha = 500$ (red).

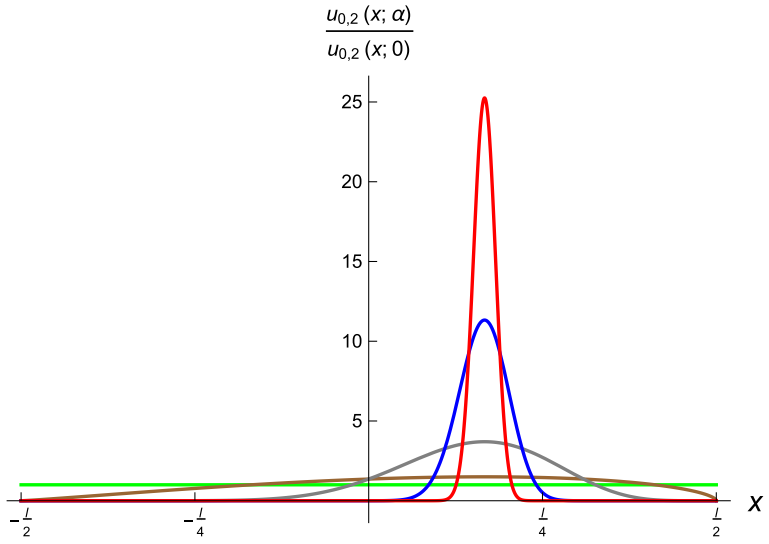

Fig. 2. Initial distributions (8) for the values $\alpha = 0$ (green, homogeneous distribution), $\alpha = 1$ (brown), $\alpha = 10$ (gray), $\alpha = 100$ (blue) and $\alpha = 500$ (red).

where $L_c = \frac{\pi}{\sqrt{\mu}}$ is the value of L corresponding at the unique nonnegative steady solution of (21), i.e.

$$\rho_s(X) = C\left(\cos(\sqrt{\mu}\,X)\right)^{\frac{1}{\mu}},$$

with C being a positive constant depending on the initial data $\rho_0(X)$. Next, we note that both survival conditions (19) and (25) can be rewritten in a unique form. Indeed, if (18) is replaced into (19) and the two sides of the resulting inequality are raised to $\mu - \nu$ (recall that $\mu > \nu$), and (22) is replaced into (25) and both sides of the resulting inequality are raised to 2, then, conditions (19) and (25) are reformulated as

$$Q \geq Q_c(\mu, \nu, \Lambda), \tag{26}$$

where Q is the parameter defined in (4) and

$$Q_c(\mu, \nu, \Lambda) = \begin{cases} N_{0,c}(\mu, \nu, \Lambda)^{\mu-\nu} & \text{if} \quad \mu > \nu, \\ \frac{\pi^2}{\mu} & \text{if} \quad \mu = \nu. \end{cases} \tag{27}$$

In terms of Q, Eq. (17) for the case $\mu > \nu$ reads

$$\int_{-\frac{1}{2}}^{\frac{1}{2}} \rho_0(X)\,dX = Q^{\frac{1}{\mu-\nu}}. \tag{28}$$

Some consequences of (4), (26) are:

1. For the particular case $\mu = \nu + 2$, the Eqs. (4), (26) do not impose any conditions on the habitat size l, but only on the total initial population n_0. Indeed, if $\mu = \nu + 2$ (and consequently $\mu > 2$) (4), (26) reads

$$n_0 \geq \sqrt{\frac{D}{a} Q_c(\mu, \mu - 2, \Lambda)}. \tag{29}$$

2. For a given total population n_0 and $\mu \in (\nu, \nu + 2)$ the Eqs. (4), (26) impose a condition on the habitat size of the form

$$l \geq l_c, \tag{30}$$

where

$$l_c = \left(\frac{D}{a} Q_c(\mu, \nu, \Lambda)\right)^{\frac{1}{-\mu+\nu+2}} n_0^{\frac{\mu-\nu}{\mu-\nu-2}}, \tag{31}$$

i.e., the population survives supposed that the habitat size is bigger than the critical size (31).

3. For a given total population n_0 and $\mu > \nu + 2$ (and consequently $\mu > 2$), the Eqs. (4), (26) impose a condition on the habitat size

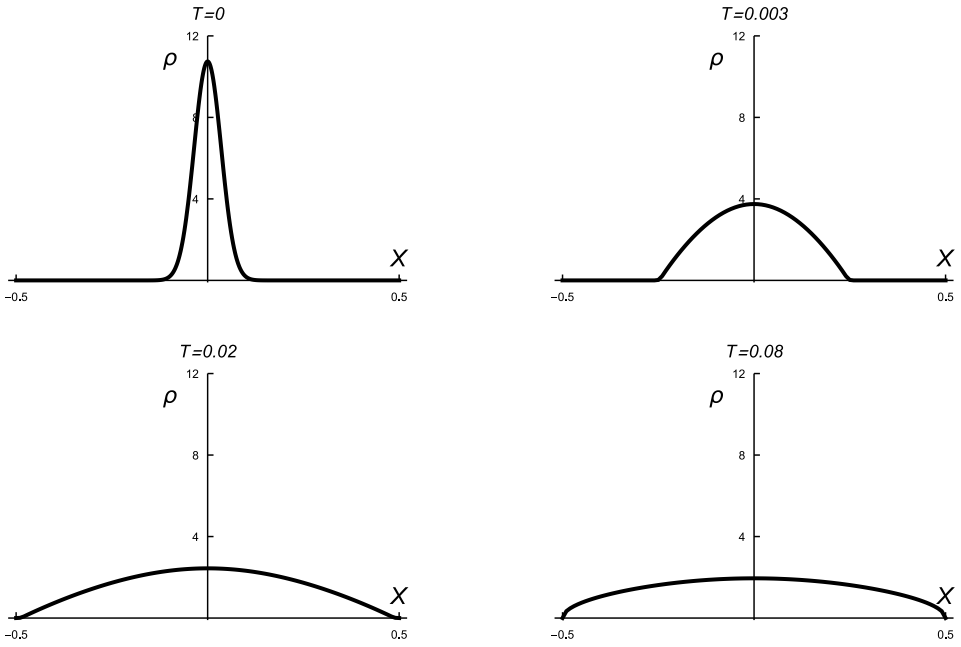

Fig. 3. Evolution of the population density governed by (15) in the nonlinear case $\mu = 4$, $\nu = 2$, when $Q = 0.9$ and initial condition (33) with $\alpha = 100$ is considered.

of the form

$$l \leq l_c, \tag{32}$$

with l_c being given by (31), i.e., the population survives supposed that the habitat size is smaller than the critical size (31).

These conclusions are in agreement with the results in [4]. However, the use of suitable nondimensional variables leads to a reformulation of the habitat problem that yields a general criterion, allowing the paradoxical situation observed in nonlinear critical-habitat models (i.e., species surviving only if the habitat is smaller than a critical size) to be expressed as the more natural condition $Q \geq Q_c(\mu, \nu, \Lambda)$, where Q combines habitat size and total initial population.

4. Results and discussion

In this section, we will make use of the numerical algorithm presented in Appendix A to determine the dependence of the critical values $Q_{c,1}(\mu, \nu, \alpha)$ and $Q_{c,2}(\mu, \nu, \alpha)$ on the values of the exponents μ, ν in the model and the parameter α in the initial conditions (7) and (8), respectively. Furthermore, we will estimate the minimum value of α for which the survival of the population is guaranteed.

In terms of the nondimensional variables, the initial condition in (15) for the case $\mu > \nu$ is determined, respectively, by (7), (16) and (4) as

$$\rho_{0,1}(X;\alpha) = \frac{Q^{\frac{1}{\mu-\nu}}}{B(1+\alpha, 1+\alpha)} \left(\frac{1}{4} - X^2\right)^{\alpha}, \tag{33}$$

or by (8), (16) and (4) as

$$\rho_{0,2}(X;\alpha) = \frac{Q^{\frac{1}{\mu-\nu}}}{B(1+\gamma(\alpha), 1+2\gamma(\alpha))} \left(\left(\frac{1}{2} - X\right)\left(\frac{1}{2} + X\right)^2\right)^{\gamma(\alpha)}, \tag{34}$$

both satisfying (28).

Analogously, the initial conditions in (21) for the case $\mu = \nu$ are given, respectively, by

$$\rho_{0,1}(X;\alpha) = \frac{Q^{-\frac{1}{2}}}{B(1+\alpha, 1+\alpha)} \left(\frac{1}{4} - \frac{X^2}{Q}\right)^{\alpha}, \tag{35}$$

and

$$\rho_{0,2}(X;\alpha) = \frac{Q^{-\frac{1}{2}}}{B(1+\gamma(\alpha), 1+2\gamma(\alpha))} \left(\left(\frac{1}{2} - \frac{X}{Q^{\frac{1}{2}}}\right)\left(\frac{1}{2} + \frac{X}{Q^{\frac{1}{2}}}\right)^2\right)^{\gamma(\alpha)}, \tag{36}$$

both satisfying (24).

4.1. Population density dynamics

Let us start by showing some illustrative examples of the behavior of the population density dynamics described by the solutions of (15) in relation to the critical values $Q_{c,1}(\mu, \nu, \alpha)$ and $Q_{c,2}(\mu, \nu, \alpha)$ for the families of initial conditions (33) and (34), respectively. Illustrative examples concerning the dynamics of the total population (in the nondimensional variables)

$$N(T) = \int_{-\frac{1}{2}}^{\frac{1}{2}} \rho(X, T)\, dX, \tag{37}$$

are provided in Appendix B.

From Section 3 we know that for a value of Q less than the corresponding critical value, the population becomes extinct (see Figs. 3 and 5), while for Q greater than the corresponding critical value, increases without limit (see Figs. 4 and 6). In order to illustrate this situation, we focus on the nonlinear case $\mu = 4$, $\nu = 2$ and $\alpha = 100$.

We observe that when the initial distribution is symmetric (33), the population density rapidly declines symmetrically, keeping its maximum value in the midpoint of the habitat, $X = 0$. After an interval of time, the situation drastically changes depending on whether $Q < Q_{c,1}(4, 2, 100)$ or $Q > Q_{c,1}(4, 2, 100)$. If $Q < Q_{c,1}(4, 2, 100)$, the population density tends to 0 at all points of the habitat size, which leads to the extinction of the given population (see Fig. 3). If $Q > Q_{c,1}(4, 2, 100)$, the population density starts growing symmetrically with respect to the midpoint of the habitat without bound (see Fig. 4).

Analogously, we observe that when the initial distribution is asymmetric (34), the population density at the original maximum location, $X = 1/6$, rapidly declines since individuals spread out across the entire habitat size in search of less crowded conditions. Once the individuals have occupied nearly the entire habitat size, the situation drastically

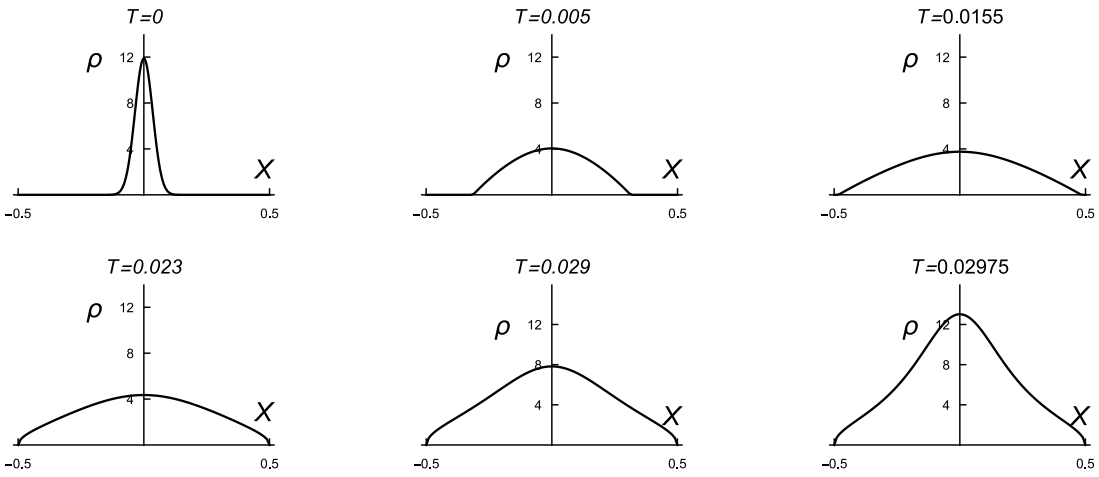

Fig. 4. Evolution of the population density governed by (15) in the nonlinear case $\mu = 4$, $\nu = 2$, when $Q = 1.1$ and initial condition (33) with $\alpha = 100$ is considered.

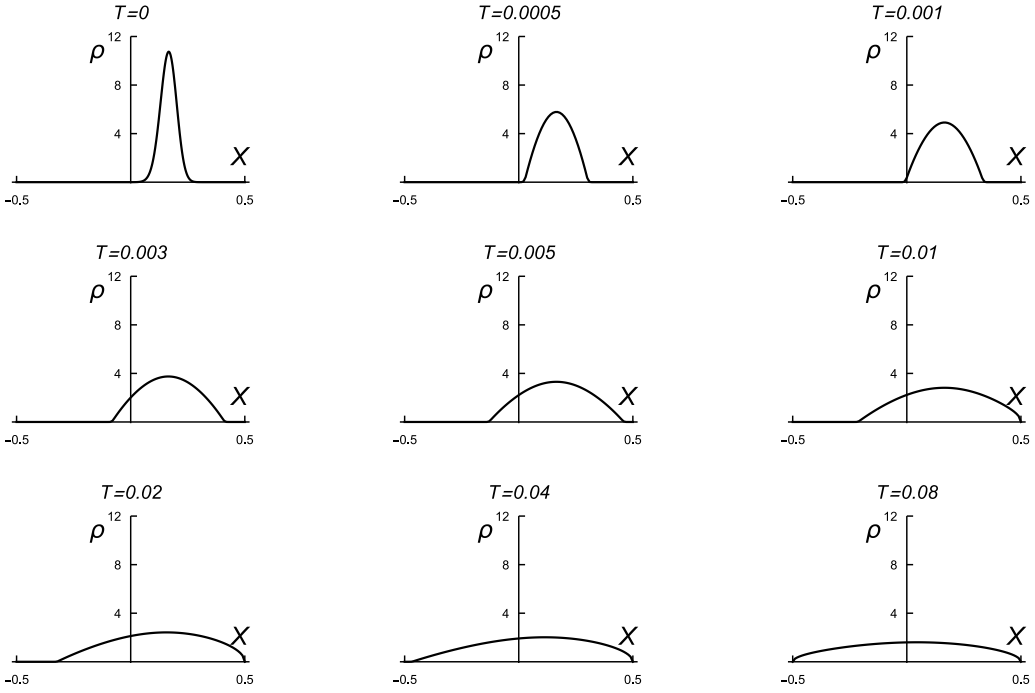

Fig. 5. Evolution of the population density governed by (15) in the nonlinear case $\mu = 4$, $\nu = 2$, when $Q = 0.9$ and initial condition (34) with $\alpha = 100$ is considered.

changes depending on whether $Q < Q_{c,2}(4, 2, 100)$ or $Q > Q_{c,2}(4, 2, 100)$. If $Q < Q_{c,2}(4, 2, 100)$, the population density tends to zero exhibiting a behavior similar to that observed when initial distribution (33) is considered with $Q < Q_{c,1}(4, 2, 100)$ (see Fig. 5). If $Q > Q_{c,2}(4, 2, 100)$, the population density grows without bound (see Fig. 6).

4.2. The critical values $Q_{c,1}(\mu, \nu, \alpha)$ and $Q_{c,2}(\mu, \nu, \alpha)$: numerical estimation

Our first goal is to apply the numerical algorithm provided in Appendix A to estimate $Q_{c,1}(\mu, \nu, \alpha)$ and $Q_{c,2}(\mu, \nu, \alpha)$ for different values of the exponents μ, ν in the model and the parameter α, respectively, in the initial conditions (33) and (34).

For simplicity of notation, we outline the procedure for estimating the critical values by considering the first family of initial conditions. Let us start by setting particular values of μ_0, ν_0, α_0 and apply the numerical algorithm to (15) where we choose $Q = Q_0$, for a certain Q_0 for the family of initial conditions (33).

We have seen that for small enough Q_0 the approximated total population, which we estimate by using the trapezoidal rule (see Appendices A and B), is an asymptotically decreasing function describing the extinction of the population, while for large enough Q_0 the total population after an interval of time turns to be a monotonically increasing function that reaches arbitrarily large values (with possible blow-up). Next, we let Q take values until we obtain two closed enough values Q^* and Q^{**} such that the approximated total population tends to zero for $Q = Q^*$ and grows without limit for $Q = Q^{**}$. To this end, we start with $Q = Q^{(0)}$ sufficiently large so that the total population becomes an increasing function once enough time has elapsed, choose a step size ΔQ sufficiently small compared with $Q^{(0)}$ and consider the sequence of values $Q^{(r)} = Q^{(r-1)} - \Delta Q$, for $r \in \mathbb{N}$. For increasing

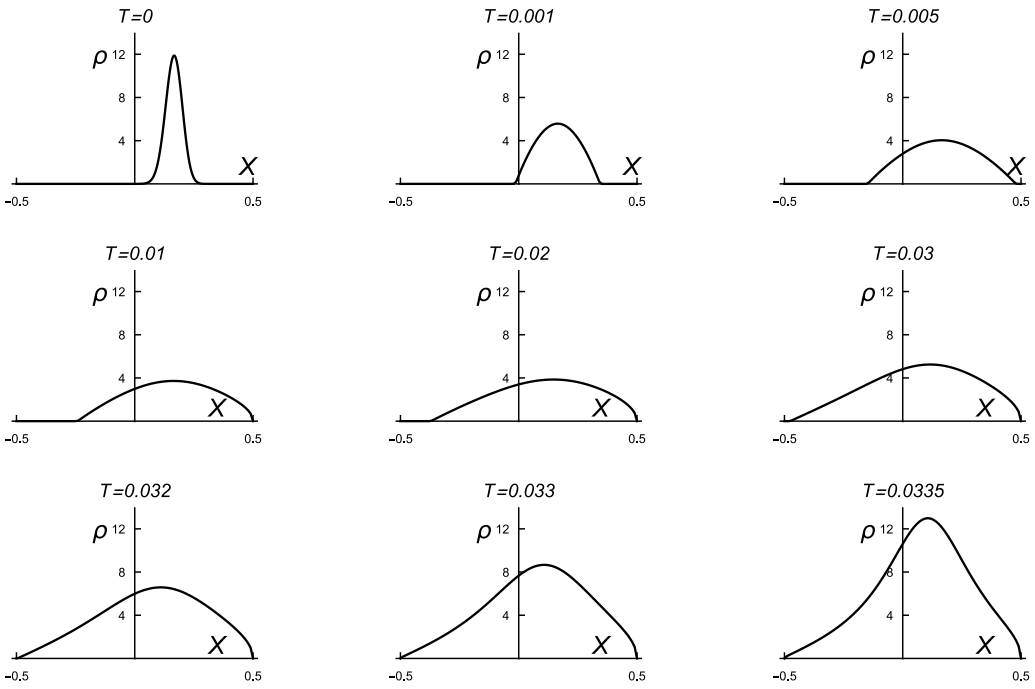

Fig. 6. Evolution of the population density governed by (15) in the nonlinear case $\mu = 4$, $\nu = 2$, when $Q = 1.1$ and initial condition (34) with $\alpha = 100$ is considered.

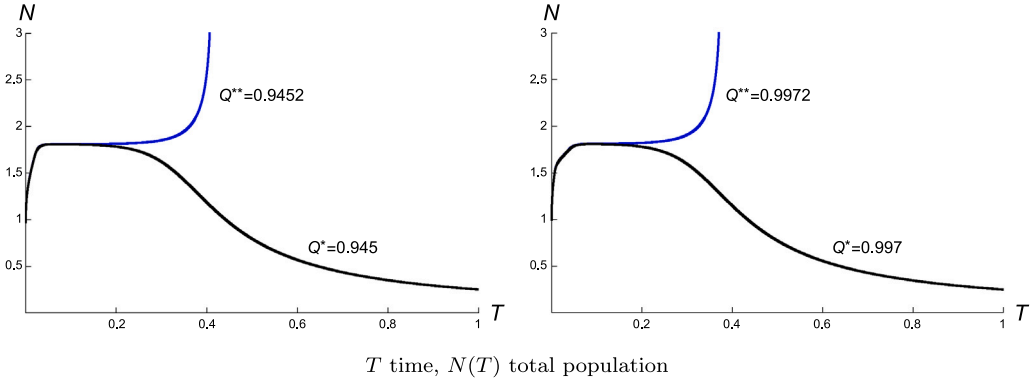

Fig. 7. Evolution of the total population for Eq. (15) with $\mu_0 = 4$, $\nu_0 = 2$, $\alpha_0 = 100$ and initial condition (33) (left) and (34) (right). The left plot shows that the total population grows for $Q^{**} = 0.9452$ (blue line) while it decreases for $Q^* = 0.945$ (black line). We estimate the critical value $Q_{c,1}(4, 2, 100) \approx 0.9451$. Similarly, from the right plot it is observed how the total population grows for $Q^{**} = 0.9972$ (blue line) while it decreases for $Q^* = 0.997$ (black line). We estimate the critical value $Q_{c,2}(4, 2, 100) \approx 0.9971$.

values of r, we apply the numerical algorithm to approximate the total population corresponding to the initial condition (33) with $Q = Q^{(r)}$. This process continues until, for a certain R, the approximated total population becomes an asymptotically decreasing function which describes the extinction of the population. We denote $Q^* = Q^{(R)}$ and $Q^{**} = Q^{(R-1)}$. Then, we approximate the critical value $Q_{c,1}(\mu_0, \nu_0, \alpha_0) \approx (Q^* + Q^{**})/2$. The same method is applied to the second family of initial conditions.

We illustrate the method for $\mu_0 = 4$, $\nu_0 = 2$ and $\alpha_0 = 100$. The choice $\Delta Q = 0.0002$ results in $Q^* = 0.945$ and $Q^{**} = 0.9452$ for the first family, and leads to $Q^* = 0.997$ and $Q^{**} = 0.9972$ for the second one. Thus, we approximate $Q_{c,1}(4, 2, 100) \approx 0.9451$ and $Q_{c,2}(4, 2, 100) \approx 0.9971$. Fig. 7 displays the approximate total population for Q^* (black lines) and Q^{**} (blue lines). The left plot corresponds to the first family of initial conditions, whereas the right plot corresponds to the second family.

Fig. 8 displays the graphs of $Q_{c,1}(\mu, 1, \alpha_0)$ (top) and $Q_{c,2}(\mu, 1, \alpha_0)$ (bottom) as functions of μ for $\alpha_0 = 0$ (green), $\alpha_0 = 1$ (brown), $\alpha_0 = 10$ (gray), $\alpha_0 = 100$ (blue) and $\alpha_0 = 500$ (red). Since $Q_{c,j}$, $j = 1, 2$, takes very small values as μ increases and α_0 assumes larger values, a logarithmic scale is particularly appropriate to enhance visual resolution at smaller values while preserving proportional relationships whereas a linear scale is suitable for small values of μ, where Q spans a wide range of values. A linear scale is used in the plots on the left whereas a logarithmic scale is used in the plots on the right. The shaded regions correspond to the survival regions in the parameter plane (μ, Q). More precisely, the green shaded region is the survival region for the homogeneous initial distribution ($\alpha_0 = 0$) and as α_0 increases the survival region enlarges progressively, adding the brown shaded region for $\alpha_0 = 1$, the gray shaded region for $\alpha_0 = 10$, the blue shaded region for $\alpha_0 = 100$ and the red shaded region for $\alpha_0 = 500$. We point out

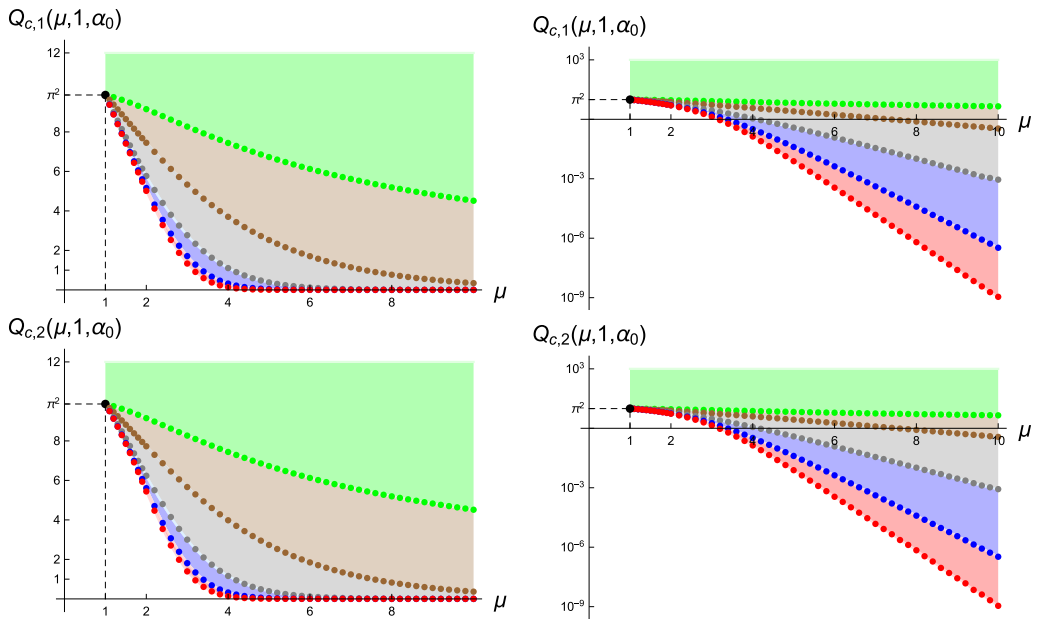

Fig. 8. Critical values $Q_{c,1}(\mu,1,\alpha_0)$ (top) and $Q_{c,2}(\mu,1,\alpha_0)$ (bottom) as functions of μ for $\alpha_0 = 0$ (green), 1 (brown), 10 (gray), 100 (blue) and 500 (red). The green shaded region corresponds to the survival region for $\alpha_0 = 0$ (i.e., the homogeneous initial distribution). As α_0 increases, the survival region enlarges, adding progressively the brown shaded region for $\alpha_0 = 1$, the gray shaded region for $\alpha_0 = 10$, the blue shaded region for $\alpha_0 = 100$ and the red shaded region for $\alpha_0 = 500$. The plots on the right are the same as those on the left, but using a logarithmic scale on the vertical axis to highlight the differences among the last three values of α_0. The black point $(1,\pi^2)$ corresponds to $Q_{c,1}(1,1,\alpha) = Q_{c,2}(1,1,\alpha) = \pi^2$ for all α.

that when the scheme to estimate $Q_{c,j}(\mu,1,\alpha_0)$ is applied to increasing values of μ, the step size ΔQ may need to be reduced ensuring that it remains sufficiently small compared to the estimated value of $Q_{c,j}(\mu,1,\alpha_0)$. It can be appreciated that, for sufficiently large values of μ (approximately $\mu \gtrapprox 4$), an increasing value of α_0 significantly reduces the critical value $Q_{c,j}(\mu,1,\alpha_0)$ and consequently facilitates population survival. However, for smaller values of μ a considerably larger α is required to achieve a noticeable reduction in $Q_c(\mu,1,\alpha_0)$, so that the strategy of using highly concentrated initial distributions becomes less effective. In particular, for $\mu = 1$ (linear case), the critical value of Q is independent of the initial distribution ($Q_{c,j}(1,1,\alpha) = \pi^2$, $j = 1,2$).

Fig. 8 also shows that the results are almost the same for both families of initial conditions. To provide a comparison between the critical values corresponding to initial conditions (33) and (34), we show in Fig. 9 the differences $Q_{c,2}(\mu,1,\alpha_0) - Q_{c,1}(\mu,1,\alpha_0)$ for $\alpha_0 = 1$ (top left), $\alpha_0 = 10$ (top right), $\alpha_0 = 100$ (bottom left) and $\alpha_0 = 500$ (bottom right). Recall that $\alpha_0 = 0$ corresponds to the homogeneous distribution for both families and consequently the results are the same.

Fig. 9 illustrates that $Q_{c,2}(\mu,1,\alpha_0) \geq Q_{c,1}(\mu,1,\alpha_0)$ for all the cases we have analyzed. However, the differences are very small when compared with the values $Q_{c,2}(\mu,1,\alpha_0)$ or $Q_{c,1}(\mu,1,\alpha_0)$. That means that initial condition (33) is slightly more propitious to ensure population survival. Note that the main difference between the two families of initial conditions is that while (33) are symmetric distributions centered at the origin, initial distributions (34) are centered in $X = 1/6$. Thus, under the initial distribution (33), individuals take, on average, the same time to reach either endpoint of the interval. In contrast, individuals initially distributed according to (34) tend to reach the right endpoint more quickly, which implies a shorter lifespan and a reduced period for reproduction. Conversely, those moving toward the left endpoint take longer to reach it, thereby enjoying a longer reproductive phase. Numerical results suggest that these opposing effects do not fully compensate each other, and the symmetric initial distribution (33) appears to be slightly more favorable in terms of population survival.

Fig. 10 displays the graphs of $Q_{c,1}(4,\nu,\alpha_0)$ as functions of ν where the same color code as in Fig. 8 is applied. Unlike Fig. 8, where all the plotted functions are monotonically decreasing, Fig. 10 shows that $Q_{c,1}(4,\nu,\alpha_0)$ decreases monotonically for $\alpha_0 = 0$ and 1, but exhibit increasing behavior for $\alpha_0 = 10$, 100 and 500. This change of behavior is related to the fact that for small diffusion exponent ν (i.e., $\nu \ll \mu = 4$) the critical value of Q is strongly reduced for larger values of α. In contrast, when ν is close to $\mu = 4$, the strategy consisting in the choice of larger values of α becomes limited.

Finally, Fig. 11 displays the graphs of $Q_{c,1}(\mu_0,1,\alpha)$ as functions of α. Fig. 11 shows that $Q_{c,1}(\mu_0,1,\alpha)$ decreases monotonically for $\mu_0 = 2$, 3 and 4. Similarly, it can be observed again that when μ_0 is close to $\nu = 1$, the approach of using larger values of α becomes less effective. Nevertheless, as μ greatly exceeds ν, higher values of α cause a significant reduction in Q.

The relationship between the critical value Q_c and α shows how the initial distribution can play a crucial role in persistence. This observation motivates the analysis in the subsequent section: determining the value of α, in order to guarantee population persistence, or equivalently, how concentrated the population must initially be to survive.

4.3. Minimum α for survival: numerical estimation

In this section, our goal is to determine the minimum value of α in the initial conditions (33) and (34) that ensures the persistence of a population whose evolution is governed by the exponents $\mu = \mu_0$ and $\nu = \nu_0$ when we assume that the habitat size is fixed and that a given total population is distributed within it. Thus, according to (4) the value of Q is fixed. Let us denote $\widehat{Q}_c(\mu_0,\nu_0) = Q_{c,1}(\mu_0,\nu_0,0) = Q_{c,2}(\mu_0,\nu_0,0)$. If $Q \geq \widehat{Q}_c(\mu_0,\nu_0)$ population survival is guaranteed, otherwise, the only adjustable parameter that can ensure survival is α. As it is shown in the previous subsection, a more concentrated initial population (i.e., larger α) increases the likelihood of persistence. Thus, for a given $Q_0 < \widehat{Q}_c(\mu_0,\nu_0)$, we look for the minimum value of α that allows population survival. We denote this threshold as $\alpha_{\min,j}(\mu_0,\nu_0,Q_0)$ where $j = 1$ for (33) and $j = 2$ for (34).

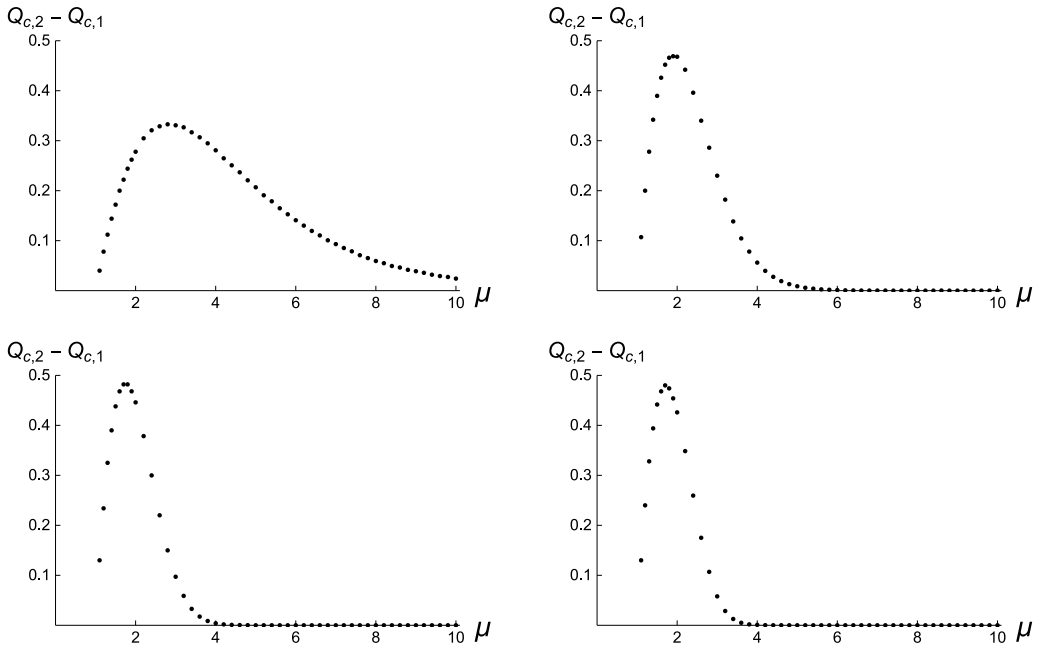

μ exponent growth term, $\nu_0 = 1$ exponent diffusion term, α_0 initial distribution parameter

Fig. 9. Differences $Q_{c,2}(\mu, 1, \alpha_0) - Q_{c,1}(\mu, 1, \alpha_0)$ between the critical values corresponding to the initial distributions (33) and (34) for $\alpha_0 = 1$ (top left), $\alpha_0 = 10$ (top right), $\alpha_0 = 100$ (bottom left) and $\alpha = 500$ (bottom right).

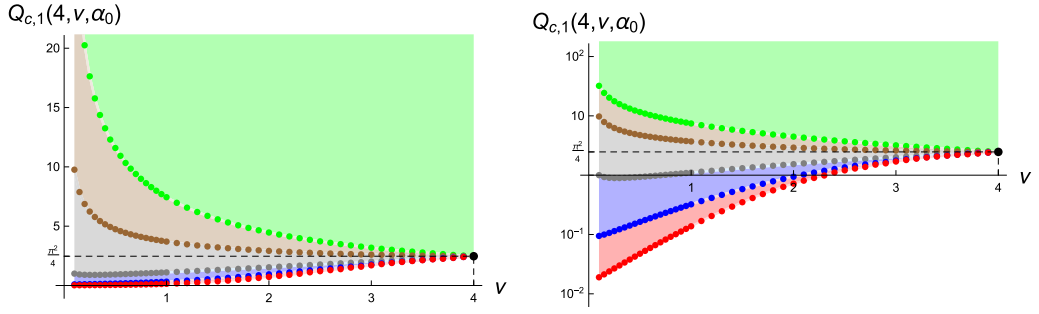

$\mu_0 = 4$ exponent growth term, ν exponent diffusion term, α_0 initial distribution parameter

Fig. 10. Critical values $Q_{c,1}(4, \nu, \alpha_0)$ as functions of ν for $\alpha_0 = 0$ (green), 1 (brown), 10 (gray), 100 (blue) and 500 (red). The green shaded region corresponds to the survival region for $\alpha_0 = 0$ (i.e., the homogeneous initial distribution). As α_0 increases, the survival region enlarges, adding progressively the brown shaded region for $\alpha_0 = 1$, the gray shaded region for $\alpha_0 = 10$, the blue shaded region for $\alpha_0 = 100$ and the red shaded region for $\alpha_0 = 500$. The plot on the right is the same as the one on the left, but using a logarithmic scale on the vertical axis to highlight the differences among the last three values of α_0. The black point $(4, \pi^2/4)$ corresponds to $Q_{c,1}(4, 4, \alpha) = \pi^2/4$ for all α.

Analogously, for simplicity of notation, we outline the procedure for estimating this cut-off value by considering the first family of initial conditions. Following the definition of $\alpha_{\min,1}(\mu_0, \nu_0, Q_0)$, we start with $\alpha^{(0)}$ large enough so that the initial condition (33) with $\alpha = \alpha^{(0)}$ leads to a total population that, after a possible transient phase, becomes a monotonically increasing function that reaches arbitrarily large values (with possible blow-up). Next, we choose a step size $\Delta\alpha$ small enough compared with $\alpha^{(0)}$ and consider the sequence of values $\alpha^{(r)} = \alpha^{(r-1)} - \Delta\alpha$, for $r \in \mathbb{N}$. For increasing values of r, we apply the numerical algorithm to approximate the total population corresponding to the initial condition (33) with $\alpha = \alpha^{(r)}$. This process continues until, for a certain R, the approximated total population becomes an asymptotically decreasing function which describes the extinction of the population. We denote $\alpha^* = \alpha^{(R-1)}$ and $\alpha^{**} = \alpha^{(R)}$ and approximate $\alpha_{\min,1}(\mu_0, \nu_0, Q_0) \approx \alpha^*$. The same method is applied to the second family of initial conditions.

We illustrate the method for $\mu_0 = 4$, $\nu_0 = 2$ and $Q_0 = 2$. Since $\widehat{Q}_c(4, 2) \approx 4.467$, it follows that $Q_0 < \widehat{Q}_c(4, 2)$. The choice $\Delta\alpha = 0.001$ results in $\alpha^* = 3.787$ and $\alpha^{**} = 3.786$ for the first family, and leads to $\alpha^* = 5.039$ and $\alpha^{**} = 5.038$ for the second one. Thus, we approximate $\alpha_{\min,1}(4, 2, 2) \approx 3.787$ and $\alpha_{\min,2}(4, 2, 2) \approx 5.039$. Fig. 12 displays the approximate total population for α^* (blue lines) and α^{**} (black lines). The left plot corresponds to the first family of initial conditions, whereas the right plot corresponds to the second family.

Fig. 13 displays the graph of $\alpha_{\min,1}(\mu_0, 1, Q)$ for $\mu_0 = 2$ (green), $\mu_0 = 3$ (blue) and $\mu_0 = 4$ (red). We point out that when the scheme to estimate $\alpha_{\min,1}(\mu_0, 1, Q)$ is applied to increasing values of Q, the step size $\Delta\alpha$ may need to be reduced ensuring that it remains sufficiently small compared to the estimated value of $\alpha_{\min,1}(\mu_0, 1, Q)$.

The red curve, represented by a set of computed points, reveals that for the exponents $\mu_0 = 4$ and $\nu_0 = 1$, even for very small values of Q, it is possible to select appropriate values of α (and consequently adopt suitable strategies to concentrate the initial population) in order to ensure population survival. The minimum required value of α to prevent extinction decreases as Q increases, tending to zero as Q approaches to $\widehat{Q}_c(4, 1) \approx 7.443$.

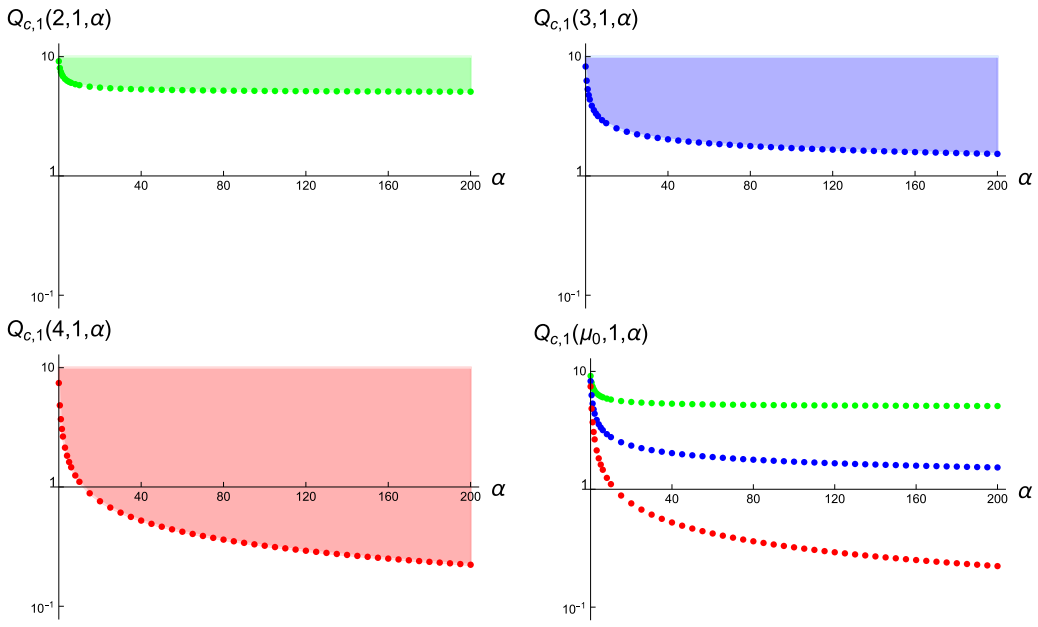

Fig. 11. Critical values $Q_{c,1}(2,1,\alpha)$ (top left), $Q_{c,1}(3,1,\alpha)$ (top right) and $Q_{c,1}(4,1,\alpha)$ (bottom left). The green shaded region corresponds to the survival region for $\mu_0 = 2$, the blue shaded region for $\mu_0 = 3$ and the red shaded region for $\mu_0 = 4$, respectively. The final plot (bottom right) combines all the obtained critical values $Q_{c,1}(\mu_0,1,\alpha)$ for the above considered values of μ_0. A logarithmic scale on the vertical axis has been used in all graphs.

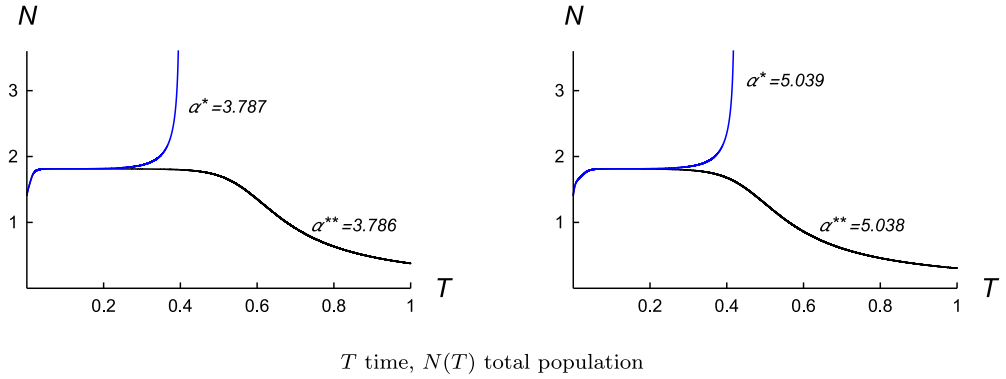

Fig. 12. Evolution of the total population for Eq. (15) with $\mu_0 = 4$, $\nu_0 = 2$, $Q_0 = 2 < \widehat{Q}_c(4,2) \approx 4.467$ and initial condition (33) (left) and (34) (right). The left plot shows that the total population grows for $\alpha^* = 3.787$ (blue line) while it decreases for $\alpha^{**} = 3.786$ (black line), which leads to $\alpha_{\min,1}(4,2,2) \approx 3.787$. Similarly, from the right plot it is observed how the total population grows for $\alpha^* = 5.039$ (blue line) and decreases for $\alpha^{**} = 5.038$ (black line), leading to $\alpha_{\min,2}(4,2,2) \approx 5.039$.

On the other hand, the blue curve indicates that for $\mu_0 = 3$ and $\nu_0 = 1$, the minimum α required for population persistence becomes very large for values of Q closed to 1 (for example $\alpha_{\min}(3,1,1.3) \approx 600.5$). Note, that very large α corresponds to an initial distribution that it is almost zero throughout the entire interval $[-\frac{1}{2},\frac{1}{2}]$ except in a very small subinterval around the origin, where the initial density reaches extremely high values. As a consequence, numerical simulations become less reliable. Moreover, it would not be realistic to assume that such an initial distribution could be practically implemented in the habitat. These observations suggest that a feasible strategy to prevent extinction can be applied for $Q \gtrapprox 1.3$. Again, $\alpha_{\min,1}(3,1,Q)$ decreases as Q increases and tends to zero as Q approaches $\widehat{Q}_c(3,1) \approx 8.269$.

A similar interpretation applies to the green curve, where $\alpha_{\min,1}(2,1,5) \approx 651.7$ and $\widehat{Q}_c(2,1) \approx 9.153$.

Note that the graphs of $\alpha_{\min,1}(\mu_0,1,Q)$ for $\mu_0 = 2$ (green), $\mu_0 = 3$ (blue) and $\mu_0 = 4$ (red) displayed in Fig. 13 are the inverse graphs of those shown in Fig. 11, with colors matching the corresponding functions for clarity.

Fig. 14 displays the graphs of $\alpha_{\min,1}(4,\nu_0,Q)$ for $\nu_0 = 1$ (red), $\nu_0 = 2$ (blue) and $\nu_0 = 3$ (green) as well as the graphs of $\alpha_{\min,2}(4,\nu_0,Q)$ for $\nu_0 = 1$ (gray), $\nu_0 = 2$ (cyan), $\nu_0 = 3$ (brown). Note that the red curve is the same as in Fig. 13. Each one of the dotted curves can be interpreted in the same way as in Fig. 13. Moreover, Fig. 14 shows that $\alpha_{\min,2}(4,\nu_0,Q)$ is slightly larger than $\alpha_{\min,1}(4,\nu_0,Q)$ for $\nu_0 = 1$ and $\nu_0 = 2$. This means that when the initial distribution is concentrated around $X = 1/6$ a slightly larger α (i.e., a slightly more concentrated initial distribution) is required to ensure population survival. In contrast, for $\nu_0 = 3$ the minimum α necessary to guarantee population persistence under the initial distribution (34) can be significantly larger than the one required when we use the initial distribution (33). These results are further illustrated in Fig. 15 where the quotient

$$\frac{\alpha_{\min,2}(4,\nu_0,Q)}{\alpha_{\min,1}(4,\nu_0,Q)}, \tag{38}$$

is displayed for $\nu_0 = 1$ (left), $\nu_0 = 2$ (middle) and $\nu_0 = 3$ (right). The figure shows that the quotient remains below 1.2 for $\nu_0 = 1$ and below 1.4 for $\nu_0 = 2$, whereas, it can reach values close to 5 for $\nu_0 = 3$.

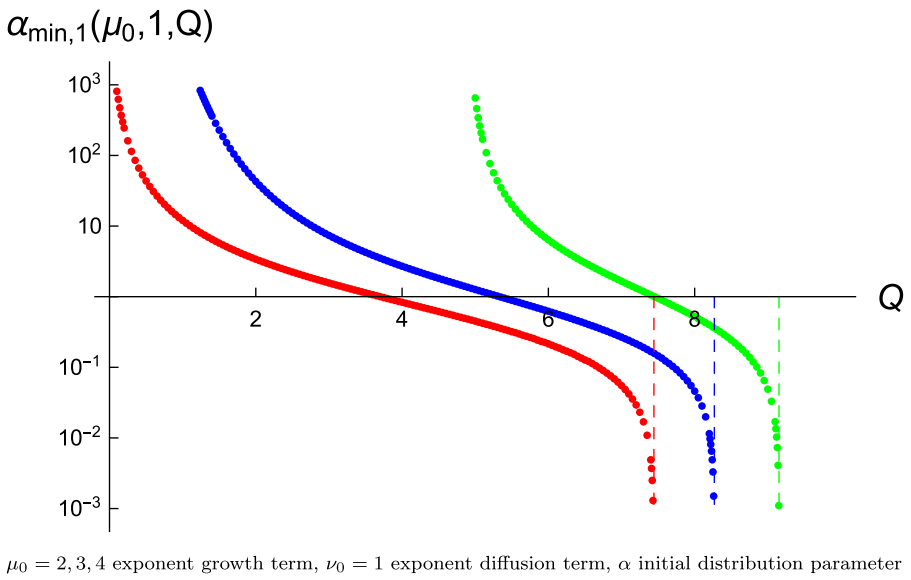

Fig. 13. Plots of $\alpha_{\min,1}(\mu_0, 1, Q)$ for $\mu_0 = 2$ (green), $\mu_0 = 3$ (blue) and $\mu_0 = 4$ (red). Logarithmic scale is used in the vertical axis so that the vertical asymptotes indicate the critical values of Q: $\widehat{Q}_c(2,1) \approx 9.153$ (green), $\widehat{Q}_c(3,1) \approx 8.269$ (blue) and $\widehat{Q}_c(4,1) \approx 7.443$ (red).

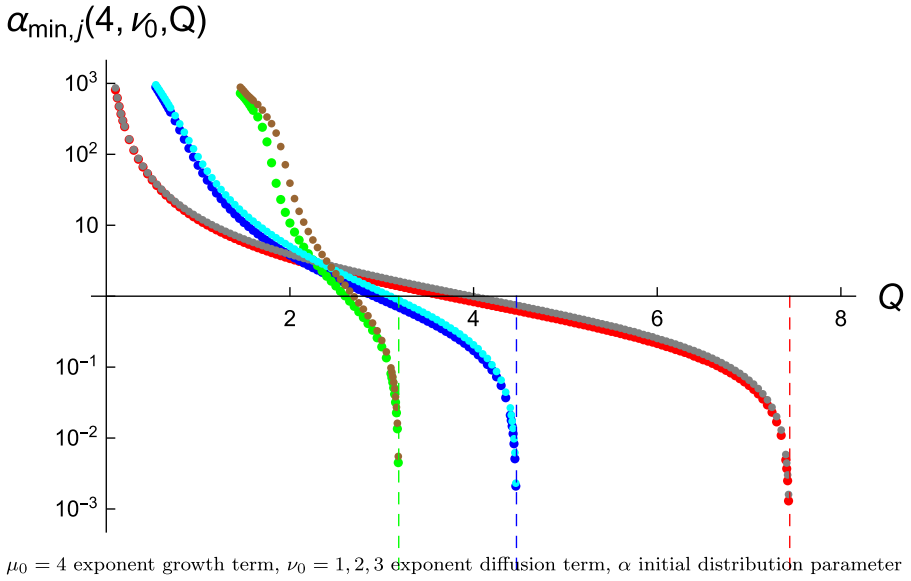

Fig. 14. Plots of $\alpha_{\min,j}(4, \nu_0, Q)$ for $j = 1$ with $\nu_0 = 1$ (red), $\nu_0 = 2$ (blue), $\nu_0 = 3$ (green) and $j = 2$ with $\nu_0 = 1$ (gray), $\nu_0 = 2$ (cyan), $\nu_0 = 3$ (brown). Logarithmic scale is used in the vertical axis so that the vertical asymptotes indicate the critical values of Q: $\widehat{Q}_c(4,1) \approx 7.443$ (red), $\widehat{Q}_c(4,2) \approx 4.467$ (blue) and $\widehat{Q}_c(4,3) \approx 3.185$ (green).

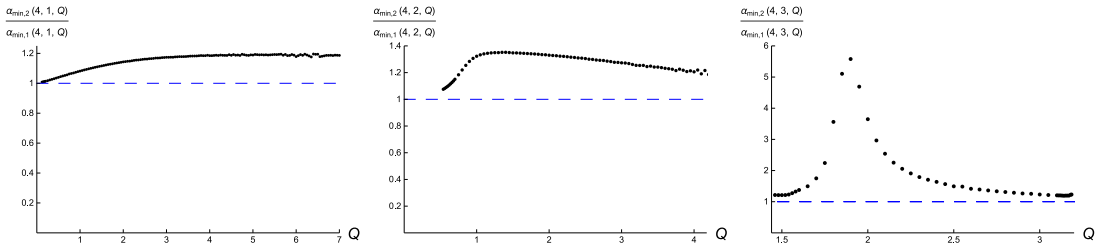

Fig. 15. Plots of the quotient $\alpha_{\min,2}(4, \nu_0, Q)/\alpha_{\min,1}(4, \nu_0, Q)$ for $\nu_0 = 1$ (left), $\nu_0 = 2$ (middle) and $\nu_0 = 3$ (right).

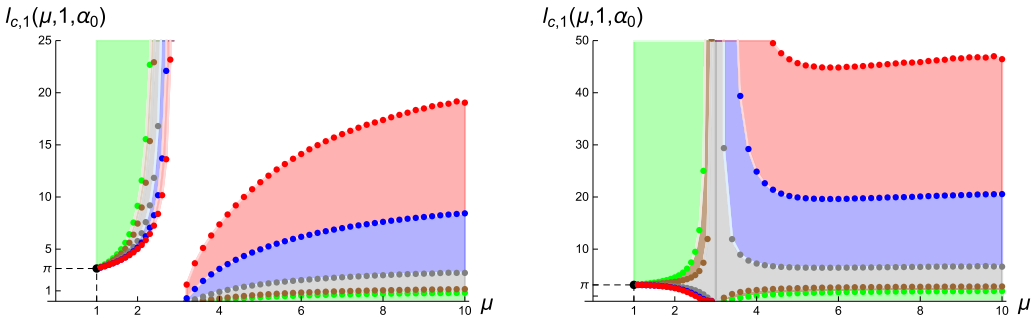

Fig. 16. Critical habitat size $l_{c,1}(\mu, 1, \alpha_0)$ for $n_0 = 1$ (left) and $n_0 = 2$ (right) as functions of μ for $\alpha_0 = 0$ (green), 1 (brown), 10 (gray), 100 (blue) and 500 (red), when $D = a = 1$. The green shaded region corresponds to the survival region for $\alpha_0 = 0$ (i.e. the homogeneous initial distribution). As α_0 increases, the survival region enlarges, adding progressively the brown shaded region for $\alpha_0 = 1$, the gray shaded region for $\alpha_0 = 10$, the blue shaded region for $\alpha_0 = 100$ and the red shaded region for $\alpha_0 = 500$. The black point $(1, \pi)$ corresponds to $l_{c,1}(1, 1, \alpha) = \pi$ for all α and n_0, when $D = a = 1$.

Finally, both Figs. 13 and 14 reveal that the choice of an appropriate α to ensure population survival for Q below $\widehat{Q}_c(\mu, \nu)$ becomes less feasible as μ and ν become closer (with $\mu > \nu$). This fact is in agreement with Eq. (27) which states that

$$Q_{c,j}(\mu, \mu, \alpha) = \frac{\pi^2}{\mu}, \quad j = 1, 2, \quad \mu > 0, \tag{39}$$

and consequently the critical value does not depend on α.

4.4. Critical habitat size and critical total population: numerical estimations

In Section 4.2 we have discussed the condition for population survival in terms of the parameter Q, defined in (4), which from the mathematical point of view, is the natural parameter to approach the problem. However, from the ecological point of view, one would be mainly interested in the conditions on either the habitat size (for a given total population) or the total population (for a given habitat size). As we have previously indicated in Section 3, the condition on the habitat size applies for μ and ν such that $\mu \neq \nu + 2$, and for our families of initial distributions takes the form

$$\begin{aligned} l &\geq l_{c,j}(\mu, \nu, \alpha) \quad \text{for} \quad \mu < \nu + 2, \quad j = 1, 2, \\ l &\leq l_{c,j}(\mu, \nu, \alpha) \quad \text{for} \quad \mu > \nu + 2, \quad j = 1, 2, \end{aligned} \tag{40}$$

with $l_{c,j}(\mu, \nu, \alpha)$ being given by

$$l_{c,j}(\mu, \nu, \alpha) = \left(\frac{D}{a} Q_{c,j}(\mu, \nu, \alpha)\right)^{\frac{1}{-\mu+\nu+2}} n_0^{\frac{\mu-\nu}{\mu-\nu-2}}. \tag{41}$$

Analogously, it is immediate to derive from (4) and (26) that the survival condition on the total population for $\mu > \nu$ and a fixed habitat size l is given by

$$n_0 \geq n_{0,c,j}(\mu, \nu, \alpha) = \left(\frac{D}{a} Q_{c,j}(\mu, \nu, \alpha)\right)^{\frac{1}{\mu-\nu}} l^{\frac{\mu-\nu-2}{\mu-\nu}}, \quad j = 1, 2. \tag{42}$$

Note that the dependences of $l_{c,j}(\mu, \nu, \alpha)$ and $n_{0,c,j}(\mu, \nu, \alpha)$ on the exponents μ and ν are considerably involved.

Fig. 16 displays the graphs of $l_{c,1}(\mu, 1, \alpha_0)$ for $n_0 = 1$ (left) and $n_0 = 2$ (right) as functions of μ for $\alpha_0 = 0$ (green), $\alpha_0 = 1$ (brown), $\alpha_0 = 10$ (gray), $\alpha_0 = 100$ (blue) and $\alpha_0 = 500$ (red), when $D = a = 1$. The shaded regions correspond to the survival regions in the parameter plane (μ, l). More precisely, the green shaded region is the survival region for the homogeneous initial distribution ($\alpha_0 = 0$) and as α_0 increases the survival region enlarges progressively, adding the brown shaded region for $\alpha_0 = 1$, the gray shaded region for $\alpha_0 = 10$, the blue shaded region for $\alpha_0 = 100$ and the red shaded region for $\alpha_0 = 500$. It is worth noting that the green shaded region in Fig. 16 (left) corresponds to Figure 5b in [4]. Furthermore, one can observe that, for sufficiently large values of μ (approximately $\mu \gtrapprox 4$ and therefore $\mu > \nu + 2$), a higher value of α_0 considerably increases the critical value $l_{c,1}(\mu, 1, \alpha_0)$ and consequently facilitates population survival. However, if $\mu < 3$ (respectively $\mu \gtrapprox 3$) a considerably larger α is required to achieve a noticeable reduction (respectively enlargement) in $l_c(\mu, 1, \alpha_0)$. When $n_0 = 2$, the situation changes drastically, increasing the survival regions for large values of α_0 in a deleted neighborhood of $\mu = 3$. This occurs, on the one hand, because for $\mu < 3$, $l_{c,1}(\mu, 1, \alpha_0)$ is a decreasing function that tends to zero as μ approaches 3 when $\alpha_0 = 10$, $\alpha_0 = 100$ and $\alpha_0 = 500$; while for μ slightly greater than 3, $l_{c,1}(\mu, 1, \alpha_0)$ takes considerably large values when $\alpha_0 = 10$, $\alpha_0 = 100$ and $\alpha_0 = 500$.

Fig. 17 displays the graphs of $l_{c,1}(4, \nu, \alpha_0)$ for $n_0 = 1$ as functions of ν using the same color code as in Fig. 16, when $D = a = 1$. As before, it should be noted that the green shaded region to the right in Fig. 17 could be compared to Figure 5a in [4], nevertheless the authors restrict their analysis to $\mu \leq 2$ and consequently, the behavior displayed on the left of Fig. 17 cannot be illustrated. For $n_0 = 1$, the behavior of $l_{c,1}(4, \nu, \alpha_0)$ compared to $l_{c,1}(\mu, 1, \alpha_0)$ differs significantly. This is due to the fact that $Q_{c,1}(4, \nu, \alpha_0)$ takes values below 1 when $\alpha_0 = 100$ and $\alpha_0 = 500$ for values of ν arbitrarily close to 2 (see Fig. 10 (right)). Consequently, $l_c(4, \nu, \alpha_0)$ attains large values when $\nu \lessapprox 2$ and small values when $\nu \gtrapprox 2$, which in turn results in a considerably expansion of the survival regions for large values of α_0 when ν approaches to 2 from either side. In contrast, when ν is close to $\mu = 4$, the strategy of considering large values of α_0 becomes limited.

Fig. 18 displays the graphs of $n_{0,c,1}(\mu, 1, \alpha_0)$ (top) for $l = 1$ (left) and $l = 5$ (right) as functions of μ, and the graphs of $n_{0,c,1}(4, \nu, \alpha_0)$ (bottom) for $l = 1$ (left) and $l = 2$ (right) as functions of ν, when $D = a = 1$, using the same color code as in Fig. 16 and with the shaded regions corresponding to the survival regions in the parameter plane (μ, n_0) (top) and the plane (ν, n_0) (bottom). A logarithmic scale is used on the vertical axis to highlight the differences among the different values of α_0. Analogously, it can be observed that when the difference between μ and ν is large (approximately $\mu \gtrapprox \nu + 3$), an increasing value of α_0 significantly reduces the critical values $n_{0,c,1}(\mu, 1, \alpha_0)$ and $n_{0,c,1}(4, \nu, \alpha_0)$, and consequently facilitates population survival. Nevertheless, when $\mu \gtrapprox \nu$ a considerably larger α is required to achieve a noticeable reduction in $n_{0,c,1}(\mu, 1, \alpha_0)$ and $n_{0,c,1}(4, \nu, \alpha_0)$, illustrating again that the strategy of using highly concentrated initial distributions becomes less effective. The variation observed between the graphs on the left and right in Fig. 18 is attributed to the factor $l^{\frac{\mu-\nu-2}{\mu-\nu}}$ appearing in expression (42).

5. Concluding remarks

We have investigated the persistence of a population evolving within a bounded habitat $[-l/2, l/2]$ according to model (5)–(6), with a particular focus on how nonlinear effects and the initial distribution shape influence the survival outcome. A central contribution of this

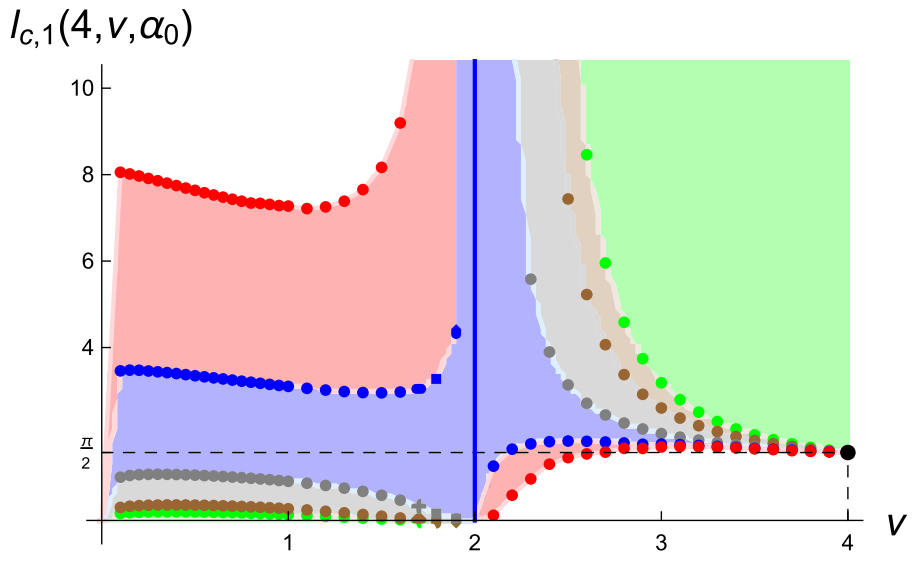

Fig. 17. Critical habitat size $l_{c,1}(4,\nu,\alpha_0)$ for $n_0 = 1$ as functions of ν for $\alpha_0 = 0$ (green), 1 (brown), 10 (gray), 100 (blue) and 500 (red), when $D = a = 1$. The green shaded region corresponds to the survival region for $\alpha_0 = 0$ (i.e., the homogeneous initial distribution). As α_0 increases, the survival region enlarges, adding progressively the brown shaded region for $\alpha_0 = 1$, the gray shaded region for $\alpha_0 = 10$, the blue shaded region for $\alpha_0 = 100$ and the red shaded region for $\alpha_0 = 500$. The black point $(4, \frac{\pi}{2})$ corresponds to $l_{c,1}(4,4,\alpha) = \frac{\pi}{2}$ for all α and n_0, when $D = a = 1$.

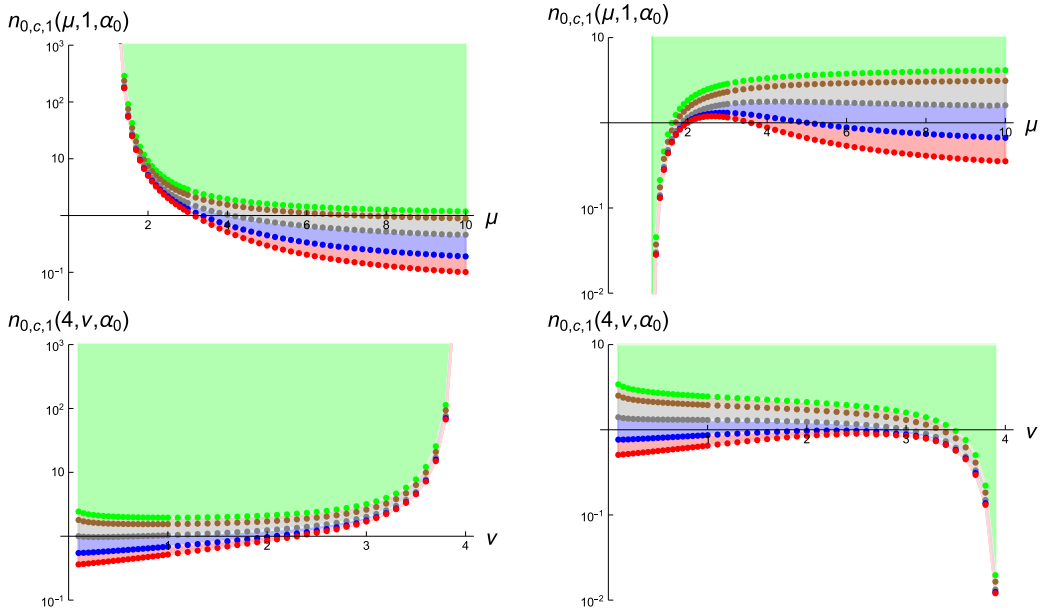

Fig. 18. Critical total initial population $n_{0,c,1}(\mu,1,\alpha_0)$ (top) for $l = 1$ (left), $l = 5$ (right) and $n_{0,c,1}(4,\nu,\alpha_0)$ (bottom) for $l = 1$ (left) and $l = 2$ (right), when $D = a = 1$. The green shaded region corresponds to the survival region for $\alpha_0 = 0$ (i.e. the homogeneous initial distribution). As α_0 increases, the survival region enlarges, adding progressively the brown shaded region for $\alpha_0 = 1$, the gray shaded region for $\alpha_0 = 10$, the blue shaded region for $\alpha_0 = 100$ and the red shaded region for $\alpha_0 = 500$. A logarithmic scale is used on the vertical axis in the plots to highlight the differences among the different values of α_0.

work is the introduction of the parameter Q (4), which provides a unified and more intuitive reformulation of the persistence question. This approach reconciles the seemingly opposite survival criteria previously reported in the literature — namely those requiring either $l > l_c$ or $l < l_c$ depending on the model exponents — by expressing persistence universally through the condition $Q \geq Q_c$ (26), where the critical value Q_c (27) depends on μ and ν as well as the initial population distribution.

To investigate the dependence of Q_c on the initial population profile, we have considered two families of distributions: one symmetric and centered at the origin (7), and another shifted toward the right boundary (8). Numerical results have been presented to analyze the

dependence of the critical values $Q_{c,j}$ on the exponents μ, ν in the model, and the parameter α in the initial conditions (7) and (8). The results computed for both families of initial conditions lead us to conclude that initial condition (7) is slightly more propitious to ensure population survival (see Fig. 9).

More importantly, we have developed a strategy to guarantee the persistence of a population whose evolution is determined by exponents $\mu = \mu_0$ and $\nu = \nu_0$, when it is assumed that the habitat size is fixed and a given total population is distributed within it. In particular, for a given $Q_0 < \widehat{Q}_c$, we have determined the minimum value of α which ensures population survival (see Figs. 13 and 14). Numerical results show that when the exponents μ and ν differ significantly, population survival is easily achieved even for small values of Q. In contrast, when the exponents μ and ν are relatively close, the minimum α required for population persistence becomes very large for small values of Q, resulting in an impractical initial distribution which is almost zero except within a very small subinterval centered at the origin (7) or at $l/6$ (8). This agrees with the fact that for $\mu = \nu$ the critical value does not depend on α.

Furthermore, by using the relationship between the habitat size (for a given total population) and Q, we have determined the critical habitat size $l_{c,j}$(41) required to ensure the survival of the population. More precisely, given a total population n_0 and $\mu \in (\nu, \nu+2)$, we have shown that the persistence of the population is guaranteed when the habitat size l is bigger than the critical size $l_{c,j}$, whereas if $\mu > \nu + 2$, the persistence of the population is guaranteed when the habitat size l is smaller than $l_{c,j}$. It is worth noting that Eqs. (4), (26) can be applied to the particular case $\mu = \nu + 2$, which was not previously considered in [4]. For this case, we have shown that Eqs. (4), (26) only impose a restriction (29) on the total initial population. Notably, the introduction of the parameter Q also reveals a significantly distinct behavior in the critical habitat size $l_{c,j}$ with respect to the total initial population n_0 (see Figs. 16 and 17).

Analogously, by using the relationship between the total initial population (for a given habitat size) with respect to $Q_{c,j}$, we have determined the minimum total initial population $n_{0,c,j}$(42) that guarantees the persistence of the population. Similarly, Fig. 18 shows the different behavior of $n_{0,c,j}$ with respect to μ, ν and l. Moreover, it can be observed again that when the exponents μ and ν differ significantly, an increasing value of α_0 substantially reduces $n_{0,c,j}$, thereby facilitating the survival of the population. Nonetheless, when μ and ν are relatively close achieving a noticeable reduction in $n_{0,c,j}$ requires a considerably larger value of α_0.

We believe that the insights provided in this work — most notably the unified formulation of the survival condition in terms of the parameter Q — establish a robust framework for interpreting conditional persistence phenomena in bounded domains. This approach contributes to a clearer understanding of how spatial constraints, intrinsic growth rates, diffusion and initial population distributions interact to determine long-term species persistence.

CRediT authorship contribution statement

Rafael de la Rosa: Writing – original draft, Visualization, Validation, Supervision, Software, Methodology, Investigation, Formal analysis, Conceptualization. **Elena Medina:** Writing – original draft, Visualization, Validation, Supervision, Software, Methodology, Investigation, Formal analysis, Conceptualization.

Declaration of competing interest

The authors declare the following financial interests/personal relationships which may be considered as potential competing interests: Rafael de la Rosa Silva reports financial support was provided by Spain Ministry of Science and Innovation. If there are other authors, they declare that they have no known competing financial interests or personal relationships that could have appeared to influence the work reported in this paper.

Acknowledgments

This work was partially supported by project PID2022-140451OA-I00 funded by Ministerio de Ciencia e Innovación, Spain/Agencia Estatal de investigación (doi:10.13039/501100011033) and by "ERDF, Spain A way of making Europe". We would like to sincerely thank the referee for the careful evaluation of our manuscript and for her/his insightful and constructive observations.

Appendix A. The numerical algorithm

Here we present the numerical algorithm used to approximate the solutions of problems (15) and (21). Let us consider the more general problem

$$\begin{cases} \rho_T = (\rho^{\nu-1}\rho_X)_X + \rho^{\mu}, & X \in \left[-\frac{L}{2}, \frac{L}{2}\right],\ T > 0, \\ \rho\left(-\frac{L}{2}, T\right) = \rho\left(\frac{L}{2}, T\right) = 0, & T > 0, \\ \rho(X,0) = \rho_0(X), & X \in \left[-\frac{L}{2}, \frac{L}{2}\right]. \end{cases} \tag{A.1}$$

Note that problem (15) is a particular case of (A.1) for $L = 1$ while (21) is a particular case of (A.1) with $\nu = \mu$. Let the solution domain of (A.1) be the closed subset of $\mathbb{R}^2$ given by

$$\Omega = \left[-\frac{L}{2}, \frac{L}{2}\right] \times \left[0, \tilde{T}\right],$$

with $\tilde{T} > 0$. Let subdivide Ω into uniform rectangular meshes formed by the intersection points, usually called grid points, of the lines $X_i = -\frac{L}{2} + ih$, $i = 0(1)m$, $T_j = jk$, $j = 0(1)n$, where $mh = L$, $nk = \tilde{T}$.

PDE in (A.1) can be written equivalently as follows

$$\rho_T = \frac{1}{\nu}(\rho^{\nu})_{XX} + \rho^{\mu}. \tag{A.2}$$

We will replace the derivatives of PDE (A.2) on each grid point by a finite-difference approximation in terms of the values of ρ at neighboring grid points. Here, we consider the finite-difference representation of PDE (A.2) given by

$$\frac{\rho_{i,j+1} - \rho_{i,j}}{k} = \frac{1}{2\nu}\left(\delta_X^2 \rho_{i,j+1}^{\nu} + \delta_X^2 \rho_{i,j}^{\nu}\right) + \rho_{i,j}^{\mu}, \tag{A.3}$$

which has been obtained by employing a forward-difference for ρ_T, the Crank–Nicolson approximation to $(\rho^{\nu})_{XX}$, and then making use of the usual central-difference operator δ_X^2 defined by

$$\delta_X^2 \rho_{i,j} = \frac{\rho_{i+1,j} - 2\rho_{i,j} + \rho_{i-1,j}}{h^2}.$$

Clearly, the finite-difference scheme (A.3) is nonlinear. Therefore, in order to linearize scheme (A.3) we apply the Richtmyer's linearization method [33,34]. Let us consider the Taylor's expansion of $\rho_{i,j+1}^{\nu}$ about the point (i, j)

$$\begin{aligned} \rho_{i,j+1}^{\nu} &= \rho_{i,j}^{\nu} + k\frac{\partial \rho_{i,j}^{\nu}}{\partial t} + \cdots \\ &= \rho_{i,j}^{\nu} + k\nu\rho_{i,j}^{\nu-1}\frac{\partial \rho_{i,j}}{\partial t} + \cdots \end{aligned}$$

Hence to terms of order k

$$\begin{aligned} \rho_{i,j+1}^{\nu} &\cong \rho_{i,j}^{\nu} + k\nu\rho_{i,j}^{\nu-1}\left(\frac{\rho_{i,j+1} - \rho_{i,j}}{k}\right) \\ &= \rho_{i,j}^{\nu} + \nu\rho_{i,j}^{\nu-1}\left(\rho_{i,j+1} - \rho_{i,j}\right), \end{aligned} \tag{A.4}$$

we can substitute the nonlinear unknown $\rho_{i,j+1}^{\nu}$ by a linear approximation in $\rho_{i,j+1}$. Similarly,

$$\begin{aligned} \rho_{i+1,j+1}^{\nu} &\cong \rho_{i+1,j}^{\nu} + \nu\rho_{i+1,j}^{\nu-1}\left(\rho_{i+1,j+1} - \rho_{i+1,j}\right) \\ \rho_{i-1,j+1}^{\nu} &\cong \rho_{i-1,j}^{\nu} + \nu\rho_{i-1,j}^{\nu-1}\left(\rho_{i-1,j+1} - \rho_{i-1,j}\right) \end{aligned} \tag{A.5}$$

Substituting (A.4) and (A.5) into scheme (A.3) and defining $W_i = \rho_{i,j+1} - \rho_{i,j}$, after some simplifications, we obtain a linear system

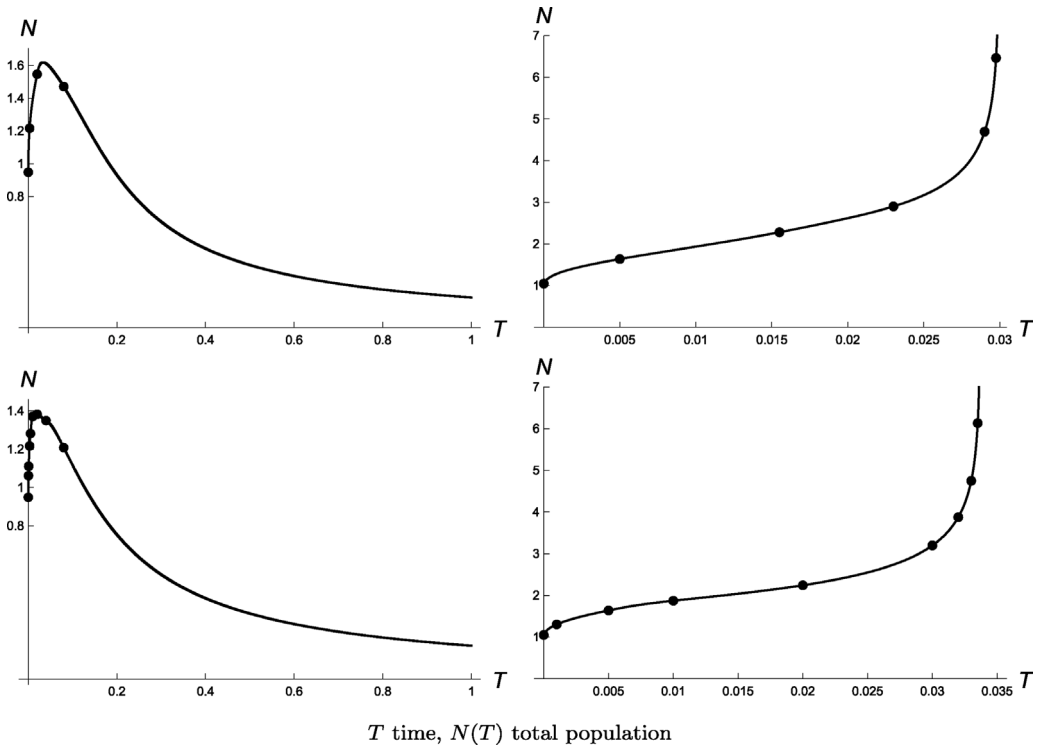

Fig. B.19. Evolution of the total population governed by (15) in the nonlinear case $\mu = 4$, $\nu = 2$ and $\alpha = 100$. The plots correspond respectively to the initial condition (33) when $Q = 0.9$ (top left) and $Q = 1.1$ (top right), and to the initial condition (34) when $Q = 0.9$ (bottom left) and $Q = 1.1$ (bottom right). Black points represent the total population size for the temporal values considered in Figs. 3, 4, 5 and 6, respectively.

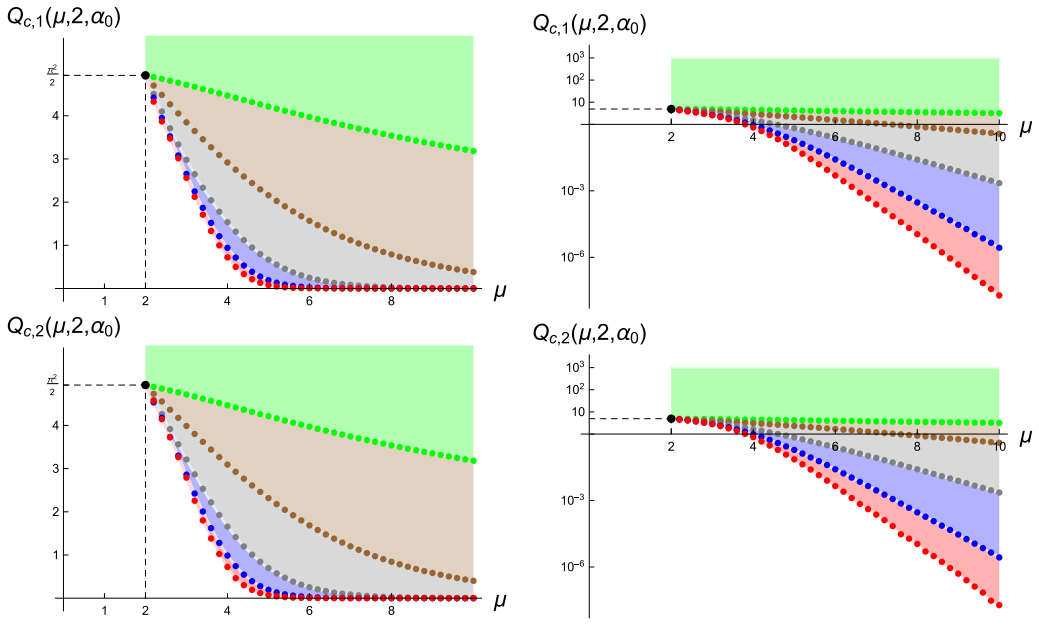

Fig. C.20. Critical values $Q_{c,1}(\mu, 2, \alpha_0)$ (top) and $Q_{c,2}(\mu, 2, \alpha_0)$ (bottom) as functions of μ for $\alpha_0 = 0$ (green), 1 (brown), 10 (gray), 100 (blue) and 500 (red). The green shaded region corresponds to the survival region for $\alpha_0 = 0$ (i.e. the homogeneous initial distribution). As α_0 increases, the survival region enlarges, adding progressively the brown shaded region for $\alpha_0 = 1$, the gray shaded region for $\alpha_0 = 10$, the blue shaded region for $\alpha_0 = 100$ and the red shaded region for $\alpha_0 = 500$. The plots on the right are the same as those on the left, but using a logarithmic scale on the vertical axis to highlight the differences among the last three values of α_0. The black point $(2, \pi^2/2)$ corresponds to $Q_{c,1}(2, 2, \alpha) = Q_{c,2}(2, 2, \alpha) = \pi^2/2$ for all α.

for W_i

$$\rho_{i+1,j}^{\nu-1}W_{i+1} - 2\left(\rho_{i,j}^{\nu-1} + \frac{h^2}{k}\right)W_i + \rho_{i-1,j}^{\nu-1}W_{i-1} = -\frac{2}{\nu}\rho_{i+1,j}^{\nu} + \frac{4}{\nu}\rho_{i,j}^{\nu} - \frac{2}{\nu}\rho_{i-1,j}^{\nu} - 2h^2\rho_{i,j}^{\mu}, \tag{A.6}$$

$i = 1(1)m-1$. The solution at the $(j+1)$th time-level is obtained from $\rho_{i,j+1} = W_i + \rho_{i,j}$.

From boundary conditions given in (A.1), we have $\rho_{0,j} = \rho_{m,j} = 0$, $\forall j$, and therefore $W_0 = W_m = 0$. Let

$$\boldsymbol{\rho^{k(j)}} = \left(\rho_{1,j}^k, \rho_{2,j}^k, \ldots, \rho_{m-1,j}^k\right)^T,$$
$$\boldsymbol{W} = \left(W_1, W_2, \ldots, W_{m-1}\right)^T.$$

Consequently, Eq. (A.6) can be written in matrix form

$$A\boldsymbol{W} = -\frac{2}{\nu}B\boldsymbol{\rho^{\nu(j)}} - 2h^2\boldsymbol{\rho^{\mu(j)}}, \tag{A.7}$$

where $A = B\,\mathrm{diag}\{\boldsymbol{\rho^{\nu-1(j)}}\} - \frac{2h^2}{k}I_{m-1}$ is a tridiagonal matrix, I_{m-1} is the unit matrix of order $m-1$ and B is given by

$$B = \begin{pmatrix} -2 & 1 & & & \\ 1 & -2 & 1 & & \\ & \ddots & \ddots & \ddots & \\ & & 1 & -2 & 1 \\ & & & 1 & -2 \end{pmatrix}.$$

Matrix system (A.7) can be solved in an efficient way by using Thomas algorithm [35].

Appendix B. Total population dynamics

The total population (37) can be estimated by using the trapezoidal rule as

$$N(j\,k) \approx h\left(\frac{\rho_{0,j}}{2} + \sum_{i=1}^{n-1}\rho_{i,j} + \frac{\rho_{n,j}}{2}\right) \quad j = 0, 1, \ldots, m. \tag{B.1}$$

In Fig. B.19, we show the temporal evolution of the total population governed by (15) for the different cases previously considered in Figs. 3, 4, 5 and 6, where black points represent the total population size for the temporal values considered in the above mentioned figures.

Appendix C. Additional numerical results

In this section, we present some additional simulations for the case $\nu_0 = 2$, which was not included in the main text for brevity. Unlike the case $\nu_0 = 1$ illustrated in Figs. 8 and 9, the case $\nu_0 = 2$ corresponds to a nonlinear diffusion term. In Fig. C.20 we show the graphs of $Q_{c,1}(\mu, 2, \alpha_0)$ (top) and $Q_{c,2}(\mu, 2, \alpha_0)$ (bottom) as functions of μ using the same color code as in Fig. 8. The graphs can be interpreted in the same way as in Fig. 8 for $\nu_0 = 1$.

Data availability

No data was used for the research described in the article.

References

[1] J.G. Skellam, Random dispersal in theoretical populations, Biometrika 38 (1/2) (1951) 196–218.
[2] S. Berti, M. Cencini, D. Vergni, A. Vulpiani, Extinction dynamics of a discrete population in an oasis, Phys. Rev. E 92 (1) (2015) 012722.
[3] R.S. Cantrell, C. Cosner, W.F. Fagan, Habitat edges and predator–prey interactions: effects on critical patch size, Math. Biosci. 175 (1) (2002) 31–55.
[4] E. Colombo, C. Anteneodo, Nonlinear population dynamics in a bounded habitat, J. Theoret. Biol. 446 (2018) 11–18.
[5] E.H. Colombo, C. Anteneodo, Population dynamics in an intermittent refuge, Phys. Rev. E 94 (4) (2016) 042413.
[6] V. Dornelas, P. de Castro, J.M. Calabrese, W.F. Fagan, R. Martinez-Garcia, Movement bias in asymmetric landscapes and its impact on population distribution and critical habitat size, in: Proceedings a, vol. 480, The Royal Society, 2024.
[7] M. Dos Santos, V. Dornelas, E.F, C. Anteneodo, Critical patch size reduction by heterogeneous diffusion, Phys. Rev. E 102 (4) (2020) 042139.
[8] E.E. Holmes, M.A. Lewis, J. Banks, R. Veit, Partial differential equations in ecology: spatial interactions and population dynamics, Ecology 75 (1) (1994) 17–29.
[9] J. Latore, P. Gould, A. Mortimer, Spatial dynamics and critical patch size of annual plant populations, J. Theoret. Biol. 190 (3) (1998) 277–285.
[10] B. Li, G. Otto, Wave speed and critical patch size for integro-difference equations with a strong allee effect, J. Math. Biol. 85 (5) (2022) 59.
[11] A.L. Lin, B.A. Mann, G. Torres-Oviedo, B. Lincoln, J. Käs, H.L. Swinney, Localization and extinction of bacterial populations under inhomogeneous growth conditions, Biophys. J. 87 (1) (2004) 75–80.
[12] D. Ludwig, D. Aronson, H. Weinberger, Spatial patterning of the spruce budworm, J. Math. Biol. 8 (3) (1979) 217–258.
[13] G.A. Maciel, R.M. Coutinho, R.A. Kraenkel, Critical patch-size for two-sex populations, Math. Biosci. 300 (2018) 138–144.
[14] T. Neicu, A. Pradhan, D. Larochelle, A. Kudrolli, Extinction transition in bacterial colonies under forced convection, Phys. Rev. E 62 (1) (2000) 1059.
[15] N. Perry, Experimental validation of a critical domain size in reaction–diffusion systems with escherichia coli populations, J. R. Soc. Interface 2 (4) (2005) 379–387.
[16] F. Xu, W. Gan, D. Tang, Population dynamics and evolution in river ecosystems, Nonlinear Anal. Real World Appl. 51 (2020) 102983.
[17] Y. Zhou, W.F. Fagan, A discrete-time model for population persistence in habitats with time-varying sizes, J. Math. Biol. 75 (2017) 649–704.
[18] Y. Jin, R. Peng, J. Wang, Enhancing population persistence by a protection zone in a reaction–diffusion model with strong allee effect, Phys. D: Nonlinear Phenom. 454 (2023) 133840.
[19] A.K. Tam, M.J. Simpson, The effect of geometry on survival and extinction in a moving-boundary problem motivated by the Fisher–KPP equation, Phys. D: Nonlinear Phenom. 438 (2022) 133305.
[20] G. Piva, E. Colombo, C. Anteneodo, Interplay between scales in the nonlocal FKPP equation, Chaos Solitons Fractals 153 (2021) 111609.
[21] V. Dornelas, E.H. Colombo, C. Anteneodo, Single-species fragmentation: The role of density-dependent feedback, Phys. Rev. E 99 (6) (2019) 062225.
[22] G. Birzu, S. Matin, O. Hallatschek, K.S. Korolev, Genetic drift in range expansions is very sensitive to density dependence in dispersal and growth, Ecol. Lett. 22 (11) (2019) 1817–1827.
[23] W.I. Newman, Some exact solutions to a non-linear diffusion problem in population genetics and combustion, J. Theoret. Biol. 85 (2) (1980) 325–334.
[24] D.J. Sumpter, The principles of collective animal behaviour, Phil. Trans. R. Soc. B 361 (1465) (2006) 5–22.
[25] J.-L. Deneubourg, S. Goss, N. Franks, A. Sendova-Franks, C. Detrain, L. Chrétien, The dynamics of collective sorting robot-like ants and ant-like robots, in: From Animals To Animats: Proceedings of the First International Conference on Simulation of Adaptive Behavior, 1991.
[26] N. Shigesada, Biological Invasions: Theory and Practice, vol. 205, Oxford University Press, 1997.
[27] J.L. Vázquez, The Porous Medium Equation: Mathematical Theory, Oxford University Press, 2007.
[28] W.I. Newman, C. Sagan, Galactic civilizations: Population dynamics and interstellar diffusion, Icarus 46 (3) (1981) 293–327.
[29] M. Mulansky, A. Pikovsky, Energy spreading in strongly nonlinear disordered lattices, New J. Phys. 15 (5) (2013) 053015.
[30] F. Courchamp, L. Berec, J. Gascoigne, Allee Effects in Ecology and Conservation, OUP Oxford, 2008.
[31] J. Gerritsen, J.R. Strickler, Encounter probabilities and community structure in zooplankton: a mathematical model, J. Fish. Board Can. 34 (1) (1977) 73–82.
[32] J.D. Murray, Mathematical Biology: I. an Introduction, vol. 17, Springer Science & Business Media, 2007.
[33] R.D. Richtmyer, K.W. Morton, Difference Methods for Initial-Value Problems, Interscience Publishers, 1967.
[34] G.D. Smith, Numerical Solution of Partial Differential Equations: Finite Difference Methods, Oxford University Press, Oxford, 1985.
[35] S.D. Conte, C. de Boor, Elementary Numerical Analysis, an Algorithmic Approach, McGraw-Hill, New York, 1972.